1 Holocene aridification trend interrupted by millennial- and centennial-scale climate
2 fluctuations from a new sedimentary record from Padul (Sierra Nevada, southern Iberian
3 Peninsula)

4 María J. Ramos-Román[1], Gonzalo Jiménez-Moreno[1], Jon Camuera[1], Antonio García-Alix[1], R.
5 Scott Anderson[2], Francisco J. Jiménez-Espejo[3], José S. Carrión[4]

6 [1] Departamento de Estratigrafía y Paleontología, Universidad de Granada, Spain
7 [2] School of Earth Sciences and Environmental Sustainability, Northern Arizona University,
8 USA.
9 [3] Department of Biogeochemistry, Japan Agency for Marine-Earth Science and Technology
10 (JAMSTEC), Japan.
11 [4] Departamento de Biología Vegetal, Facultad de Biología, Universidad de Murcia, Murcia,
12 Spain.

13 *Correspondence to:* María J. Ramos-Román (mjrr@ugr.es)

14 **Abstract.** Holocene centennial-scale paleoenvironmental variability has been described in a
15 multiproxy analysis (i.e. lithology, geochemistry, macrofossil and microfossil analyses) of a
16 paleoecological record from the Padul basin in Sierra Nevada, southern Iberian Peninsula. This
17 sequence covers a relevant time interval hitherto unreported in the studies of the Padul
18 sedimentary sequence. The ca. 4700 yr-long record has preserved proxies of climate variability,
19 with vegetation, lake levels and sedimentological change the Holocene in one of the most unique
20 and southernmost peat bogs from Europe. The progressive Middle and Late Holocene trend
21 toward arid conditions identified by numerous authors in the western Mediterranean region,
22 mostly related to a decrease in summer insolation, is also documented in this record, being here
23 also superimposed by centennial-scale variability in humidity. In turn, this record shows
24 centennial-scale climate oscillations in temperature that correlate with well-known climatic
25 events during the Late Holocene in the western Mediterranean region, synchronous with
26 variability in solar and atmospheric dynamics. The multiproxy Padul record first shows a
27 transition from a relatively humid Middle Holocene in the western Mediterranean region to more
28 aridity from ~4700 to ~2800 cal yr BP. A relatively warm and humid period occurred between
29 ~2600 to ~1600 cal yr BP, coinciding with persistent negative NAO conditions and the historic
30 Iberian-Roman Humid Period. Enhanced arid conditions, co-occurring with overall positive
31 NAO conditions and increasing solar activity, are observed between ~1550 to ~ 450 cal yr BP
32 (~400 to ~1400 CE) and colder and warmer conditions happened during the Dark Ages and
33 Medieval Climate Anomaly, respectively. Slightly wetter conditions took place during the end of
34 the MCA and the first part of the Little Ice Age, which could be related to a change towards
35 negative NAO conditions and minima in solar activity. Evidences of higher human impact in the
36 Padul peat bog area are observed in the last ~1550 cal yr BP. Time series analysis performed
37 from local (*Botryococcus* and TOC) and regional signals (Mediterranean forest) helped us
38 determining the relationship between southern Iberian climate evolution, atmospheric, oceanic
39 dynamics and solar activity.

40 **Keywords:** Holocene, Padul**,** peat bog, North Atlantic Oscillation, atmospheric dynamics,
41 southern Iberian Peninsula, Sierra Nevada, western Mediterranean.

1 Introduction

The Mediterranean area is situated in a sensitive region between temperate and subtropical climates making it an important place to study the connections between atmospheric and oceanic dynamics and environmental changes. Climate in the western Mediterranean and the southern Iberian Peninsula is influenced by several atmospheric and oceanic dynamics (Alpert et al., 2006), including the North Atlantic Oscillation (NAO) one of the principal atmospheric phenomenon controlling climate in the area (Hurrell, 1995; Moreno et al., 2005). Recent NAO reconstructions in the western Mediterranean region relate negative and positive NAO conditions with an increase and decrease in winter (effective) precipitation, respectively (e.g. Olsen et al., 2012; Trouet et al., 2009). Numerous paleoenvironmental studies in the western Mediterranean have detected a link at millennial- and centennial-scales between the oscillations of paleoclimate proxies studied in sedimentary records with solar variability and atmospheric (i.e., NAO) and/or ocean dynamics during the Holocene (e.g. Fletcher et al., 2013; Moreno et al., 2012; Rodrigo-Gámiz et al., 2014). Very few montane and low altitude lake records in southern Iberia document centennial-scale climate change [see, for example Zoñar Lake (Martín-Puertas et al., 2008)], with most terrestrial records in the western Mediterranean region evidencing only millennial-scale cyclical changes. Therefore, higher-resolution decadal-scale analyses are thus necessary in order to analyze the link between solar activity, atmospheric and oceanographic systems with terrestrial environment in this area at shorter (ie., centennial) time scales.

Sediments from lakes, peat bogs and marine records from the western Mediterranean have documented an aridification trend during the Late Holocene (e.g. Carrión et al., 2010b; Gil-Romera et al., 2014; Jalut et al., 2009). This trend, however, was superimposed by shorter-term climate variability, as shown by several recent studies from the region, as well as human pressure (Carrión, 2002; Fletcher et al., 2013; Jiménez-Moreno et al., 2013; Martín-Puertas et al., 2008; Ramos-Román et al., 2016). This relationship between climate variability, culture evolution and human impact during the Late Holocene has also been the subject of recent paleoenvironmental studies (Carrión et al., 2007; Lillios et al., 2016; López-Sáez et al., 2014; Magny, 2004). However, it is still unclear what has been the main forcing driving environmental change (i.e., deforestation) in this area during this time: was it climate or humans?

Within the western Mediterranean region, Sierra Nevada is the highest and southernmost mountain range in the Iberian Peninsula and thus presents a critical area for paleoenvironmental studies. Most high-resolution studies there have come from high elevation sites. The well-known Padul peat bog site is located at the western foot of the Sierra Nevadas (Fig. 1) and bears one of the longest continental records in southern Europe, with a sedimentary sequence of ca. 100 m thick that could represent the last 1 Ma (Ortiz et al., 2004). Several research studies, including radiocarbon dating, geochemistry and pollen analyses, have been carried out on previous cores from Padul, and have documented glacial/interglacial cycles during the Pleistocene and up until the Middle Holocene. However, the Late Holocene section of the Padul sedimentary sequence has never been retrieved and studied. This was due to the location of these previous corings within the peat mine exploitation setting, where the upper (and non productive) part of the sedimentary sequence was missing (Florschütz et al., 1971; Ortiz et al., 2004; Pons and Reille, 1988).

Here we present a new record from the Padul peat bog basin: Padul-15-05, a 42.64 m-long sediment core that, for the first time, contains a continuous record of the Late Holocene (Fig. 2). A high-resolution multi-proxy analysis of the upper 1.15 m, the past ~4700 cal yr BP, has allowed us to determine a complete paleoenvironmental and paleoclimatic record at centennial-

88 and millennial-scales. To accomplish that, we reconstructed changes in the Padul peat bog
89 vegetation, ~~sedimentation,~~ climate and human impact during the Holocene throughout the
90 interpretation of the lithology, palynology and geochemistry.
91 Specifically, the main objective of this paper is to determine environmental variability and
92 climate evolution in the southern Iberian Peninsula and the western Mediterranean region and
93 their linkages to northern hemisphere climate and solar variability during the Holocene. In order
94 to do this, we compared our results with other paleoclimate records from regional areas and solar
95 activity from the northern hemisphere for the past ca. 4.7 cal ka BP (Bond et al., 2001; Laskar et
96 al., 2004; Sicre et al., 2016; Steinhilber et al., 2009).

2   Study site

2.1 Regional setting: Sierra Nevada climate and vegetation

99   Sierra Nevada is a W-E aligned mountain range located in Andalusia (southern Spain). Climate
100 in this area is Mediterranean, with cool and humid winters and hot/warm summer drought. In the
101 Sierra Nevada, the mean annual temperature at approximately 2500 m asl is 4.5 ºC and the mean
102 annual precipitation is 700 mm/yr (Oliva et al., 2009). Sierra Nevada is strongly influenced by
103 thermal and precipitation variations due to the altitudinal gradient (from ca. 700 to more than
104 3400 m), which control plant taxa distribution in different bioclimatic vegetation belts due to the
105 variability in thermotypes and ombrotypes (Valle Tendero, 2004). According to the
106 climatophilous series classification, Sierra Nevada is divided in four different vegetation belts
107 (Fig. 1). The crioromediterranean vegetation belt, occurring above ~2800 m, is characterized
108 principally by *Festuca clementei*, *Hormatophylla purpurea*, *Erigeron frigidus*, *Saxifraga*
109 *nevadensis*, *Viola crassiuscula*, and *Linaria glacialis*. The oromediterranean belt, between ~1900
110 to 2800 m, bears *Pinus sylvestris*, *P. nigra*, *Juniperus communis subsp. hemisphaerica*, *J. sabina*
111 var. *humilis*, *J. communis* subsp. *nana*, *Genista versicolor*, *Cytisus oromediterraneus*,
112 *Hormatophylla spinosa*, *Prunus prostrata*, *Deschampsia iberica* and *Astragalus sempervirens*
113 subsp. *nevadensis* as the most representative species. The supramediterranean belt, from
114 approximately 1400 to 1900 m of elevation, principally includes *Quercus pyrenaica*, *Q. faginea*,
115 *Q. rotundifolia*, *Acer opalus* subsp. *granatense*, *Fraxinus angustifolia*, *Sorbus torminalis*,
116 *Adenocarpus decorticans*, *Helleborus foetidus*, *Daphne gnidium*, *Clematis flammula*, *Cistus*
117 *laurifolius*, *Berberis hispanicus*, *Festuca scariosa*, *Thymus serpylloides* subsp. *gadoriensis*,
118 *Helichrysum italicum* subsp. *serotinum*, *Santolina rosmarinifolia* subps. *canescens* and *Artemisia*
119 *glutinosa*. The mesomediterranean vegetation belt occurs between ~600 and 1400 m of elevation
120 and is characterized by *Quercus rotundifolia*, *Retama sphaerocarpa*, *Paeonia coriacea*,
121 *Juniperus oxycedrus*, *Rubia peregrina*, *Asparagus acutifolius*, *D. gnidium*, *Ulex parviflorus*,
122 *Genista umbellata*, *Cistus albidus* and *C. lauriflolius* (Al Aallali et al., 1998; Valle, 2003). The
123 human impact over this area, especially important during the last millennium, affected the
124 natural vegetation distribution through fire, deforestation, cultivation. (i.e., *Olea*) and subsequent
125 reforestation (mostly *Pinus)* (Anderson et al., 2011).

2.2 Padul peat bog

127 The Padul basin is situated at approximately 725 m of elevation in the southeastern part of the
128 Granada Basin, at the foothill of the southwestern Sierra Nevada, Andalucía, Spain (Fig. 1). This
129 is one of the most seismically active areas in the southern Iberian Peninsula with numerous faults

130 in NW-SE direction, with the Padul fault being one of these active normal faults (Alfaro et al.,
131 2001). It is a small extensional basin approximately 12 km long and covering an area of
132 approximately 45 km^2, which is bounded by the Padul normal fault. The sedimentary in-filling of
133 the basin consists of Neogene and Quaternary deposits; Upper Miocene conglomerates,
134 calcarenites and marls, and Pliocene and Quaternary alluvial sediments, lacustrine and peat bog
135 deposits (Sanz de Galdeano et al., 1998; Delgado et al., 2002; Domingo et al., 1983). The Padul
136 peat bog is an endorheic area with a surface of approximately 4 km^2 placed in the Padul basin
137 that contains a sedimentary sequence mostly characterized by peat. The basin fill is asymmetric,
138 with thicker peat infill to the northeast (~100 m thick; Domingo-García et al., 1983; Florschütz et
139 al., 1971; Nestares and Torres, 1997) and disappearing to the southwest (Alfaro et al., 2001). The
140 main source area of the sediments in the Padul peat bog is Sierra Nevada, which is characterized
141 at higher elevations by Paleozoic siliceous metamorphic rocks (mostly mica-schists and
142 quartzites) from the Nevado-Filabride complex and, at lower elevations and acting as bedrock,
143 by Triassic dolomites, limestones and phyllites from the Alpujárride Complex (Sanz de
144 Galdeano et al. 1998). Geochemistry in the Padul sediments is influenced by detritic materials
145 coming from the neighboring mountains, mainly the Sierra Nevada mountain range (Ortiz et al.,
146 2004). In addition, groundwater inputs into the Padul basin are the main reason why there is a
147 wetland in this area. These inputs come from the Triasic carbonates aquifers (N and S edge to the
148 basin), the out–flow of the Granada Basin (W) and the conglomerate aquifer to the east edge
149 (Castillo Martín et al., 1984; Ortiz et al., 2004). The main water output is by evaporation and
150 evapotranspiration, water wells and by canals ("madres") that drain the water to the Dúrcal river
151 to the southeast (Castillo Martín et al., 1984). Climate in the Padul area is characterized by a
152 mean annual temperature of 14.4 ºC and a mean annual precipitation of 445 mm
153 (http://www.aemet.es/).
154 Vegetation in the Padul area is dominated by *Q. rotundifolia* (and in less amounts *Q. faginea*),
155 which is normally accompanied by *Pistacia terebinthus*. Shrub species in the area include
156 *Juniperus oxycedrus*, *Crataegus monogyna*, *Daphne gnidium* and *Ruscus aculeatus*. Creepers
157 such as *Lonicera implexa*, *Rubia peregrina*, *Hedera helix*, *Asparagus acutifolius* also occur in
158 this area and some herbs, such as *Paeonia broteroi*. *Quercus coccifera* also occurs in crests and
159 very sunny rocky outcrops. *Retama sphaerocarpa* and *Genista cinerea* subsp. *speciosa* and the
160 *Thymo-Stipetum tenacissime* series also occur in sunny areas and in more xeric soils.
161 Nitrophilous communities occur in soils disrupted by livestock, pathways or open forest,
162 normally related with anthropization (Valle, 2003).
163 The Padul-15-05 drilling site was located around 50 m south of the present-day Padul lake shore
164 area. This basin area is presently subjected to seasonal water level fluctuations and is principally
165 dominated by *Phragmites australis* (Poaceae). The lake environment is dominated by aquatic
166 and wetland communities with *Chara vulgaris*, *Myriophyllum spicatum, Potamogeton*
167 *pectinatus, Potamogetum coloratus*, *Phragmites australis, Typha dominguensis*, *Apium*
168 *nodiflorum, Juncus subnodulosus, Carex hispida, Juncus bufonius* and *Ranunculus muricatus*
169 between others (Pérez Raya and López Nieto, 1991). Some sparse riparian trees occur in the
170 northern lake shore, such as *Populus alba*, *Populus nigra*, *Salix* sp., *Ulmus minor* and *Tamarix*.

171 **3 Material and methods**

172 Two sediment cores, Padul-13-01 (37º00'40''N; 3º36'13''W) and Padul-15-05 (37º00'39.77''N;
173 3º36'14.06''W) with a length of 58.7 cm and 42.64 m, respectively, were collected between
174 2013 and 2015 from the peat bog (Fig. 1). The cores were taken using a Rolatec RL-48-L drilling

175 machine equipped with a hydraulic piston corer from the Scientific Instrumentation Centre of the
176 University of Granada. The sediment cores were wrapped in film, put in core boxes, transported
177 and stored in a dark cool room at +4ºC.

3.1 Age-depth model (AMS radiocarbon dating)

179 The core chronology was constrained using fourteen AMS radiocarbon dates from plant remains
180 and organic bulk samples taken throughout the cores (Table 1). In addition, one sample with
181 gastropods was also measured for AMS radiocarbon analysis, although it was rejected due to
182 important reservoir effect, which provide a very old date. Thirteen of these samples came from
183 Padul-15-05 and one from the nearby Padul-13-01 (Table 1). We were able to use this date from
184 Padul-13-01 core as there is a very significant correlation between the upper part of Padul-15-05
185 and Padul-13-01 cores, shown by identical lithological and geochemical changes (Supplementary
186 information 1; Figure S1). The age model for the upper ~3 m until 21 cm from the surface was
187 built using the R-code package 'Clam 2.2' (Blaauw, 2010) employing the calibration curve
188 IntCal 13 (Reimer et al., 2013), a 95 % of confidence range, a smooth spline (type 4) with a 0.20
189 smoothing value and 1000 iterations (Fig. 2). The chronology of the uppermost 21 cm of the
190 record was built using a linear interpolation between the last radiocarbon date and the top of the
191 record (Present; 2015 CE). The studied interval in the present work are the uppermost 115 cm of
192 the record that are constrained by six AMS radiocarbon dates (Fig. 2).

3.2 Lithology, MS, XRF and TOC

194 The length for the Padul-15-05 core is ~ 43 m. In this study, we focus in the uppermost ~ 115 cm
195 from that core. Padul-15-05 core was split longitudinally and was described in the laboratory
196 with respect to lithology and color (Fig. 3).
197 Magnetic susceptibility (MS) was measured with a Bartington MS3 operating with a MS2E
198 sensor. MS measurements (in SI units) were obtained directly from the core surface every 0.5 cm
199 (Fig. 3).
200 Elemental geochemical composition was measured in an X-Ray fluorescence (XRF) Avaatech
201 core scanner® at the University of Barcelona (Spain). A total of thirty-three chemical elements
202 were measured in the XRF core scanner at 10 mm of spatial resolution, using 10 s count time, 10
203 kV X-ray voltage and a X-ray current of 650 μA for lighter elements and 35 s count time, 30 kV
204 X-ray voltage, X-ray current of 1700 μA for heavier elements. Thirty-three chemical elements
205 were measured but only the most representative with a major number of counts were considered
206 (Si, K, Ca, Ti, Fe, Zr, Br and Sr). Results for each element are expressed as intensities in counts
207 per second (cps) and normalized (norm.) for the total sum in cps in every measure (Fig. 3).
208 Total organic carbon (TOC) was analyzed every 2 or 3 cm throughout the core. Samples were
209 previously decalcified with 1:1 HCl in order to eliminate the carbonate fraction. The percentage
210 of organic Carbon (OC %) was measured in an Elemental Analyzer Thermo Scientific Flash
211 2000 model from the Scientific Instrumentation Centre of the University of Granada (Spain).
212 Percentage of TOC per gram of sediment was calculated from the percentage of organic carbon
213 (OC %) yielded by the elemental analyzer, and recalculated by the weight of the sample prior to
214 decalcification (Fig. 3).

3.3 Pollen and NPP

216   Samples for pollen analysis (1-3 cm³) were taken every 1 cm throughout the core. Pollen
217   extraction methods followed a modified Faegri and Iversen (1989) methodology. Processing
218   included the addition of *Lycopodium* spores for calculation of pollen concentration. Sediment
219   was treated with NaOH, HCl, HF and the residue was sieved at 250 mm previous to an acetolysis
220   solution. Counting was performed using a transmitted light microscope at 400 magnifications to
221   an average pollen count of ca. 260 terrestrial pollen grains. Fossil pollen was identified using
222   published keys (Beug, 1961) and modern reference collections at University of Granada (Spain).
223   Pollen counts were transformed to pollen percentages based on the terrestrial pollen sum,
224   excluding aquatics. The palynological zonation was executed by cluster analysis using twelve
225   different pollen taxa- *Olea*, *Pinus* undifferentiated, deciduous *Quercus*, evergreen *Quercus*,
226   *Pistacia*, Ericaceae, *Artemisia*, Asteroideae, Cichorioideae, Amaranthaceae and Poaceae
227   (Grimm, 1987) (Fig. 4). Non-pollen palynomorphs (NPP) include fungal and algal spores, and
228   thecamoebians (testate amoebae). The NPP percentages were calculated and represented with
229   respect to the terrestrial pollen sum (Fig. 4). Furthermore, some pollen taxa were grouped,
230   according to present-day ecological bases, in Mediterranean forest and xerophytes (Fig. 4). The
231   Mediterranean forest taxa is composed of *Quercus* total, *Olea*, *Phillyrea* and *Pistacia*. The
232   xerophyte group includes *Artemisia*, *Ephedra*, and Amaranthaceae.

233   4 Results

234   4.1 Chronology and sedimentation rates

235   The age-model of the studied Padul-15-05 core (Fig. 2) shows that the top 115 cm continuously
236   cover approximately the last ca. 4700 cal yr BP, being the age constrained by fourteen AMS ¹⁴C
237   dates (Table 1). Five distinct sediment accumulation rate (SAR) intervals can be differentiated
238   between 0 and 122.96 cm based on the linear interpolation between radiocarbon dates in the
239   studied core (Fig. 2).

240   4.2 Lithology, MS, XRF and TOC

241   The lithology of the upper ca. 115 cm of the Padul-15-05 sediment core was mainly deduced
242   from a visual inspection together with the element geochemical composition (XRF) and the
243   correlation of these data, and the MS of the split cores. In addition, this information was
244   complemented with the TOC (Fig. 3).
245   A Linear r (Pearson) correlation was calculated for the XRF data, the correlation for the
246   inorganic geochemical elements show us two different groups of elements that covary (Table 2):
247   Group 1) Si, K, Ti, Fe and Zr with a high positive correlation between them; Group 2) Ca, Br
248   and Sr have negative correlation with Group 1. The lithology for this sedimentary sequence
249   consists in clays with variable carbonates, siliciclastics and organic content (Fig. 3). Based on
250   this, the sequence is subdivided in two principal sedimentary units. The bottom of the record
251   corresponds with Unit 1, characterized principally by lower values of MS and higher values of
252   Ca. The top of the sequence can be subdivided in Unit 2, in which the mineralogical composition
253   is lower in Ca with higher values of MS in correlation with mostly siliciclastics elements (Si, K,
254   Ti, Fe and Zr). Within these two units, four different facies can be identified by visual inspection
255   and by the elemental geochemical composition and TOC of the sediments. *Facies* 1, between
256   115-110 cm depth (ca. 4700 to 4650 cal yr BP) and 89-80 cm depth (ca. 4300 to 4000 cal yr BP),
257   are characterized by dark brown organic clays that bear charophytes and plant remains. They are

258 also depicted by relative higher values of TOC values (Fig. 3). *Facies* 2, between 110-89 cm
259 depth (ca. 4650 to 4300 cal yr BP) and 80-42 cm depth (ca. 4000 to 1600 cal yr BP), are made up
260 of brown clays, with the occurrence of gastropods and charophytes. These are also characterized
261 with decreasing TOC values. *Facies* 3, between 42-28 cm depth (ca. 1600 to 450 cal yr BP), are
262 characterized by grayish brown clays with the occurrence of gastropods, and lower values of
263 TOC, the increasing trend in MS and in siliciclastic elements. *Facies* 4, between 28-0 cm/ ca.
264 450 cal yr BP to Present, are made up of light grayish brown clays and feature a strong increase
265 in siliciclastic linked to a strong increase in MS.

266 4.3 Pollen and NPP

267 A total of seventy-two pollen taxa were identified but only the most representative ~~taxa~~ are here
268 plotted in a summary pollen diagram (Fig. 4). Selected NPP percentages are also displayed in
269 Figure 4. Four pollen zones (Fig. 4) were visually identified with the help of a cluster analysis
270 using the program CONISS (Grimm, 1987). Pollen zones are described below:

271 4.3.1 Zone Padul-15-05-1 [~4720 to 3400 cal yr BP/ ~2800 to 1450 BCE (115-65 cm)]

272 Zone 1 is characterized by the abundance of Mediterranean forest species reaching up to ca. 70
273 %. Another important taxon in this zone is *Pinus,* with average values around 18 %. Herbs are
274 largely represented by Poaceae, averaging around 10 %, and reaching up to ca. 25 %. This pollen
275 zone is subdivided into subzones-1a, 1b and 1c (Fig. 4). The principal characteristic that
276 differentiate subzone-1a to subzone-1b (boundary at ca. 4650 cal yr BP/ca. 2700 BCE) is the
277 decrease in Poaceae from an average value of ca. 18 to 10 %, the increase in *Pinus* from ca. 7 to
278 18 %, and the appearance of cf. *Vitis.* The decrease in Mediterranean forest to average values
279 around 40 %, the increase in *Pinus* to average values around 25 % and a progressive increase in
280 Ericaceae with average occurrences from ca. 6 to 11 %, allow to discern subzones 1b and 1c
281 (boundary at ca. 3950 cal yr BP).

282 4.3.2. Zone Padul-15-05-2 [~3400 to 1550 cal yr BP/~1450 BCE to 400 CE (65-41 cm)]

283 The main features of this zone are the increase in Ericaceae up to ca. 16 % and in deciduous
284 *Quercus*, reaching values around 20 %. Therefore, the Mediterranean forest component
285 progressively decreased to values around 34 %. Some herbs such as Cichorioideae became more
286 abundant reaching average occurrences around 7 %. This pollen zone can be subdivided in
287 subzones 2a and 2b with a boundary at ~2850 cal yr BP (~900 BCE). The principal
288 characteristics that differentiate these subzones is marked by the increase in Mediterranean forest
289 types and the increasing trend in deciduous *Quercus* and Ericaceae. The increase in
290 *Botryococcus* averages ca. 4 to 9 % and the expansion of *Mougeotia and Zygnema* type are also
291 noticeable.

292 4.3.3 Zone Padul-15-05-3 [~1550 to 450 cal yr BP/~400 CE to 1500 CE (41-29 cm)]

293 This zone is distinguished by the maximum depletion of Mediterranean forest elements.
294 Cichorioideae reached average values of about 40 %. The decrease in Ericaceae is also
295 significant. A decrease in *Botryococcus* and other algal remains is observed in this zone,
296 although there is an increase in other Thecamoebians from average values <1 % to 10 %. This
297 pollen zone is subdivided in subzones 3a and 3b at ~1000 cal yr BP (~950 CE). The main

298 features that differentiate these subzones are the increase in *Olea* from subzone 3a to 3b from
299 average values of ca. 1 to 5 %. The increasing trend in Poaceae is also a feature in this subzone,
300 as well as the slight increase in Asteroideae at the top. Significant changes are documented in
301 NPP percentages in this subzone with the expansion of some fungal remain such as *Tilletia* and
302 *Glomus* type. Furthermore, a decrease in *Botrycoccus* and the near disappearance of other algal
303 remains such as *Mougetia* occurred.

4.3.4 Zone Padul-15-05-4 [~last 450 cal yr BP/ ~ 1500 CE to Present (29-0 cm)]

305 The main feature in this zone is the significant increase in *Pinus,* reaching maximum values (ca.
306 32 %), an increase in Poaceae (ca. 40 %) and the decrease in Cichorioideae (from average
307 occurrences of ca. 44 to 16 %). Other important changes are the nearly total disappearance of
308 some shrubs such as *Pistacia* and a decreasing trend in Ericaceae, as well as an important
309 decrease in Mediterranean forest pollen. An increase in wetland pollen taxa, mostly *Typha* also
310 occurred. A significant increase in xerophytes, with the expansion of Amaranthaceae to ~14 %,
311 is also observed in this period. Other herbs such as *Plantago*, Polygonaceae and Convolvulaceae
312 show moderate increases. This zone 4 is subdivided into subzones 4a and 4b (Fig. 4). The top of
313 the record, which corresponds approximately 1830 CE to Present, is characterized by the
314 subzone 4b, the main characteristic that differentiate subzone 4b from the previous 4a is a
315 decrease in some herbs such as Cichorioideae. However, an increase in some xerophytic herbs
316 such as Amaranthaceae occurred. The increase in *Plantago* is also significant during this period.
317 A noteworthy increase in *Pinus* (from an average of ca. 14 to 27 %) and a slight increase in *Olea*
318 and evergreen *Quercus* are also characteristic of this subzone. With respect to NPP, there is an
319 increase in thecamoebians such as *Arcella* type and in the largely coprophilous sordariaceous
320 (Sordariales) group. This zone also documents the decrease in fresh-water algal spores, in
321 *Botryococcus* concomitant with *Mougeotia and Zygnema type.*

4.4 Estimated lake level reconstruction

323 Different local proxies from the Padul-15-05 record [Si, Ca, TOC, MS, Hygrophytes (made up of
324 Cyperaceae and ~~Typha~~), Poaceae and Algae (including Botryoccocus, Zygnema type
325 and Mougeotia) groups] have been depicted in order to understand the relationship between
326 lithological, geochemical, and palynological variability and the water lake level oscillations.
327 Sediments with higher values of TOC (more algae and hygrophytes), rich in Ca (related with the
328 occurrence of shells and charophytes remains) most likely characterized a shallow water
329 environment. The absence of aquatic shells, decreasing Ca and a lower TOC and/or a higher
330 input of clastic material (higher MS and Si values) into the lake, could be related with lake level
331 lowering, and a shallower wetland environment (increase in Poaceae) (Fig. 5).

4.5 Spectral analysis

333 Spectral analysis was performed on selected pollen and NPP time series (Mediterranean forest
334 and *Botryococcus)*, as well as TOC in order to identify millennial- and centennial-scale
335 periodicities in the Padul-15-05 record. The mean sampling resolution for pollen and NPP is ca.
336 50 yr and for geochemical data is ca. 80 yr. Statistically significant cycles, above the 90, 95 and
337 99 % of confident levels, were found around 800, 680, 300, 240, 200, 170 (Fig. 7).

5 Discussion

338

339 Different proxies have been used in this study to interpret the paleoenvironmental and
340 hydrodynamic changes recorded in the Padul peat bog sedimentary record during the last 4700
341 cal yr BP. Palynological analysis (pollen and NPP) is commonly used as a proxy for climate
342 change, lake level variations and human impact and land uses (e.g. Faegri and Iversen, 1990; van
343 Geel et al., 1983). In this study, we used the variations between Mediterranean forest taxa,
344 xerophytes and algal communities for paleoclimatic variability and the occurrence of
345 nitrophilous and ruderal plant communities and some NPPs for identifying human influence in
346 the study area (Fig. 4). Variations in arboreal pollen (AP, including Mediterranean tree species)
347 have previously been used in the Sierra Nevada records as a proxy for humidity changes
348 (Jiménez-Moreno and Anderson, 2012; Ramos-Román et al., 2016). The abundance of the
349 Mediterranean forest has been used as a proxy for climate change in other studies in the western
350 Mediterranean region, with higher forest development generally meaning higher humidity
351 (Fletcher et al., 2013; Fletcher and Sánchez-Goñi, 2008). On the other hand, increases in
352 xerophyte pollen taxa (i.e., *Artemisia*, *Ephedra*, Amaranthaceae) have been used as an indication
353 of aridity in this area (Anderson et al., 2011; Carrión et al., 2007).
354 The chlorophyceae alga *Botryococcus* sp. has been described as an indicator of freshwater
355 environments, in relatively productive fens, temporary pools, ponds or lakes (Guy-Ohlson,
356 1992). The high visual and statistical correlation between *Botryococcus* from Padul-15-05 and
357 North Atlantic temperature estimations (Bond et al., 2001; r = -0.63; *p* < 0.0001; between ca.
358 4700 to 1500 cal ka BP – the decreasing and very low *Botryococcus* occurrence in the last 1500
359 cal yr BP makes this correlation moderate: r=-0.48; *p* < 0.0001 between 4700 and -65 cal yr BP)
360 seems to show that in this case *Botryococcus* is driven by temperature change and would reflect
361 variations in lake productivity (increasing with warmer water temperatures).
362 In addition to the palynological analysis, variations in the lithology, geochemistry and
363 macrofossil remains (gastropod shells and charophytes) from the Padul-15-05 core helped us
364 reconstruct the estimated lake level and the local environment changes in the Padul peat bog.
365 Several previous studies on Late Holocene lake records from the Iberian Peninsula show that
366 lithological changes can be used as a proxy for lake level reconstruction (Martín-Puertas et al.,
367 2011; Morellón et al., 2009; Riera et al., 2004). For example, carbonate sediments formed by
368 biogenic remains of gastropods and charophytes are indicative of shallow lake waters (Riera et
369 al., 2004). Furthermore, van Geel et al. (1983), described occurrences of *Mougeotia* and
370 *Zygnema* type (Zygnemataceae) as typical of shallow water environments. The increase in
371 organic matter accumulation deduced by TOC (and Br) could be considered as characteristic of
372 high productivity (Kalugin et al., 2007) in these shallow water environments. On the other hand,
373 increases in clastic input in lake sediments have been interpreted as due to lowering of lake level
374 and more influence of terrestrial-fluvial deposition in a very shallow/ephemeral lake (Martín-
375 Puertas et al., 2008). We used the variations between those proxies to estimate water level (Fig.
376 5).
377 Nitrophilous and ruderal pollen taxa (*Convolvulus*, *Plantago lanceolata* type, Urticaceae type
378 and/or *Polygonum avicularis* type) are also very useful as proxies for human impact (Riera et al.,
379 2004). Some species of Cichorioideae have also been described in different studies from the
380 Iberian Peninsula as nitrophilous taxa (Abel-Schaad and López-Sáez, 2013). At the same time,
381 NPP taxa such as some coprophilous fungi, Sordariales and thecamoebians are also used as
382 indicators of anthropization and land use (Carrión et al., 2007; Ejarque et al., 2015; van Geel et
383 al., 1989; Riera et al., 2006). *Tilletia* a grass-parasitizing fungi has been described as an indicator

384   of grass cultivation in other Iberian records (Carrión et al., 2001b). In this study we also used the
385   NPP mycorrhizal fungus *Glomus* sp. as a proxy for erosive activity. This interpretation comes
386   from a study from van Geel et al. (1989), who correlated erosive events with elevated
387   percentages of *Glomus* cf. *fasciculatum*.

5.1 Late Holocene aridification trend

389   This study shows that a progressive aridification trend occurred during at least the last ca. 4700
390   cal yr BP in the southern Iberian Peninsula. The increase in aridity is shown in the Padul-15-05
391   core by a progressive decrease in Mediterranean forest component and the increase in herbs
392   (Figs. 4 and 7). Lake level interpretations from our record agree with the pollen and show an
393   overall decrease during the Late Holocene, from a shallow water table containing relatively
394   abundant organic matter (high TOC, indicating higher productivity), gastropods and charophytes
395   (high Ca values) to a low-productive ephemeral/emerged environment (high clastic input and MS
396   and decrease in Ca) (Fig. 5). This progressive aridification confirmed by the increase in
397   siliciclastics pointing to a change towards ephemeral (even emerged) environments became more
398   prominent since the last ca. 1550 cal yr BP and then enhanced again in the last 300 cal yr BP to
399   Present. *Glomus*, a spore from mycorrhizal fungi that occur in soils (van Geel et al., 1989),
400   follows a similar pattern of change, which probably points to enhanced soil erosion in the
401   catchment area during the last 1550 cal yr BP. Furthermore, the increase in some proxies
402   indicating human land use during this last period suggests that humans were more active in this
403   area since then.
404   These results are supported by previous studies from the Mediterranean area using different
405   proxies documenting an aridification trend since the Middle Holocene (Carrión, 2002; Carrión et
406   al., 2010a; Fletcher et al., 2013; Fletcher and Sánchez-Goñi, 2008; Jiménez-Espejo et al., 2014;
407   Jiménez-Moreno et al., 2015). In the western Mediterranean region this decline in forest
408   development during the Middle and Late Holocene is related with a decrease in summer
409   insolation (Fletcher et al., 2013; Jiménez-Moreno and Anderson, 2012). This would produce a
410   progressive cooling, with a reduction in the length of the growing season as well as a decrease in
411   the sea-surface temperature (Marchal et al., 2002), generating a decrease in the land-sea contrast
412   that would be reflected in a reduction of the wind system and a reduced precipitation gradient
413   from sea to shore during the fall-winter season. Also, a reorganization of the general atmospheric
414   circulation with a northward shift of the westerlies - a long-term enhanced positive NAO trend -
415   has been interpreted, inducing drier conditions in this area since 6000 cal yr BP (Magny et al.,
416   2012). The aridification trend can clearly be seen in the nearby alpine records from the Sierra
417   Nevada, where there was little influence by human activity (Anderson et al., 2011; Jiménez-
418   Moreno et al., 2013; Jiménez-Moreno and Anderson, 2012; Ramos-Román et al., 2016).

**5.2 Millennial- and centennial-scale climate variability in the Padul peat bog during the
Late Holocene**

421   The multi-proxy paleoclimate record from Padul-15-05 shows an overall aridification trend.
422   However, this trend seems to be modulated by millennial- and centennial-scale climatic
423   variability.

**5.2.1 Aridity pulses around 4200 (4500, 4300 and 4000 cal yr BP) and around 3000 cal yr
BP (3300 and 2800 cal yr BP)**

426 Marked aridity pulses are registered in the Padul-15-05 record around 4200 and 3000 cal yr BP
427 (Unit 1; Pollen zones 1 an 2a; Figs. 6 and 7). These arid pulses are mostly evidenced in this
428 record by declines in Mediterranean forest taxa, as well as lake level drops and/or cooling
429 evidenced by a decrease in organic component as TOC and the decrease in *Botryococcus* algae.
430 However, a discrepancy between the local and regional occurs between 3000-2800 cal yr BP,
431 with an increase in the estimated lake level and a decrease in the Mediterranean forest during the
432 late Bronze Age until the early Iron Age (Figs. 6 and 7). The disagreement could be due to
433 deforestation by humans during a very active period of mining in the area observed as a peak in
434 lead pollution in the alpine records from Sierra Nevada (García-Alix et al., 2013) . The aridity
435 pulses agree regionally with recent studies carried out at higher in elevation in the Sierra Nevada,
436 a decrease in AP percentage in Borreguil de la Caldera record around 4000-3500 cal yr BP
437 (Ramos-Román et al., 2016), high percentage of non-arboreal pollen around 3400 cal ka BP in
438 Zoñar lake [Southern Córdoba Natural Reserve; (Martín-Puertas et al., 2008)], and lake
439 desiccation at ca. 4100 and 2900 cal yr BP in Lake Siles (Carrión et al., 2007). Jalut et al. (2009)
440 compared paleoclimatic records from different lakes in the western Mediterranean region and
441 also suggested a dry phase between 4300 to 3400 cal yr BP, synchronous with this aridification
442 phase. Furthermore, in the eastern Mediterranean basin other pollen studies show a decrease in
443 arboreal pollen concentration toward more open landscapes around 3.7 ka cal BP (Magri, 1999).
444 Significant climatic changes also occurred in the Northern Hemisphere at those times and polar
445 cooling and tropical aridity are observed at ca. 4200-3800 and 3500-2500 cal yr BP; (Mayewski
446 et al., 2004), cold events in the North Atlantic [cold event 3 and 2; (Bond et al., 2001)], decrease
447 in solar irradiance (Steinhilber et al., 2009) and humidity decreases in the eastern Mediterranean
448 area at 4200 cal yr BP (Bar-Matthews et al., 2003) that could be related with global scale climate
449 variability (Fig. 6). These generally dry phases between 4.5 and 2.8 in Padul-15-05 are generally
450 in agreement with persistent positive NAO conditions during this time (Olsen et al., 2012).
451 The high-resolution Padul-15-05 record shows that climatic crises such as the one occurred at ca.
452 4200 cal yr BP, which seems to be recorded worldwide (Booth et al., 2005), are the product of
453 the sum of more than one single climatic event (i.e., ca. 4500, 4300, 4000 cal yr BP) and thus are
454 affected by climatic variability at centennial-scales.

5.2.2 Iberian-Roman Humid Period (~2600 to 1600 cal yr BP)

456 High relative humidity is recorded in the Padul-15-05 record between ca. 2600 and 1600 cal yr
457 BP, synchronous with the well-known Iberian-Roman Humid Period (IRHP; between 2600 and
458 1600 cal yr BP; (Martín-Puertas et al., 2009). This is interpreted in our record due to an increase
459 in the Mediterranean forest species at that time (Unit 1; Pollen Zone 2.b; Figs. 6 and 7). In
460 addition, there is a simultaneous increase in *Botryococcus* algae, which is probably related to
461 higher productivity during warmer conditions. Evidence of a wetter climate around this period
462 has also been shown in other regional records and several alpine records from Sierra Nevada. For
463 example, Jiménez-Moreno et al. (2013) studying a sediment record from the Laguna de la Mula,
464 showed an increase in deciduous *Quercus* in correlation with the maximum in algae between
465 2500 to 1850 cal yr BP, also evidencing the most humid period of the Late Holocene. A
466 geochemical study from the Laguna de Río Seco (also in Sierra Nevada) also evidenced humid
467 conditions around 2200 cal yr BP by the decrease in Saharan dust input and the increase in
468 detritic sedimentation into the lake suggesting higher rainfall (Jiménez-Espejo et al., 2014). In
469 addition, Ramos-Román et al. (2016) showed an increase in AP in the Borreguil de la Caldera
470 record around 2200 cal yr BP, suggesting an increase in humidity at that time.

471 Other records from the Iberian Peninsula also show this pattern to wetter conditions during the
472 IRHP. For example, high lake levels are recorded in Zoñar Lake in southern Spain between 2460
473 to 1600 cal yr BP, only interrupted by a relatively arid pulse between 2140 and 1800 cal yr BP
474 (Martín-Puertas et al., 2009). An increase in rainfall is described in the central region of the
475 Iberian Peninsula in a study from the Tablas de Daimiel National Park between 2100 and 1680
476 cal yr BP (Gil García et al., 2007). Deeper lake levels at around 2650 to 1580 cal yr BP, also
477 interrupted by an short arid event at ca. 2125-1790 cal yr BP, were observed to the north, in the
478 Iberian Range (Currás et al., 2012). The fact that the Padul-15-05 record also shows a relatively
479 arid-cold event between 2150-2050 cal yr BP, just in the middle of this relative humid-warm
480 period, seems to point to a common feature of centennial-scale climatic variability in many
481 western Mediterranean and North Atlantic records (Fig. 6). Humid climate conditions at around
482 2500 cal yr BP are also interpreted in previous studies from lake level reconstructions from
483 Central Europe (Magny, 2004). Increases in temperate deciduous forest are also observed in
484 marine records from the Alboran Sea around 2600 to 2300 cal yr BP, also pointing to high
485 relative humidity (Combourieu Nebout et al., 2009; Fletcher et al., 2007). Overall humid
486 conditions between 2600 and 1600 cal yr BP seem to agree with predominant negative NAO
487 reconstructions at that time, which would translate into greater winter (and thus more effective)
488 precipitation in the area triggering more development of forest species in the area.
489 Generally warm conditions are interpreted between 1900 and 1700 cal yr BP in the
490 Mediterranean Sea, with high sea surface temperatures (SSTs), and in the North Atlantic area,
491 with the decrease in Drift Ice Index. In addition, persistent positive solar irradiance occurred at
492 that time. The increase in *Botryococcus* algae reaching maxima during the IRHP also seems to
493 point to very productive and perhaps warmer conditions in the Padul peat bog area (Fig. 6).

494 **5.2.3 DA and MCA – aridity between ~1550 cal yr BP and 600 cal yr BP**

495 Enhanced aridity occurred right after the IRHP in the Padul peat bog area between ca. 1550 and
496 600 cal yr BP (ca. 400 - 1350 CE). This is deduced in the Padul-15-05 record by a significant
497 forest decline, with a prominent decrease in Mediterranean forest, an increase in Cichorioideae
498 herbs and the decline in the estimated water level (Unit 1; Pollen Zone 3; Figs. 4 and 7). A
499 significant change since the end of the IRHP took place in the lake environment, suggesting the
500 transition from a shallow water table to an ephemeral environment. This is deduced by the
501 disappearance of charophytes, a significant decrease in Algae component and higher Si and MS
502 and lower TOC values (Unit 1; Figs. 6 and 7).
503 This arid phase could be separated into two different periods. The first period occurred between
504 ca. 1550 cal yr BP (ca. 400 CE) and ca. 1100 cal yr BP (ca. 900 CE) and is characterized by a
505 decreasing trend in Mediterranean forest and *Botryococcus* taxa and the increase in
506 Cichorioideae. This period corresponds with the Dark Ages [from ca. 500 to 900 CE; (Moreno et
507 al., 2012)]. A visual correlation between the decrease in Mediterranean forest, the increase in the
508 Drift Ice Index in the North Atlantic record (cold event 1; Bond et al., 2001), the decrease in
509 SSTs in the Mediterranean Sea and maxima in positive NAO reconstructions suggests drier and
510 colder conditions during this time (Fig. 6). Other Mediterranean and central-European records
511 agree with our climate interpretations, for example, a decrease in forest extent is shown in a
512 marine record from the Alboran Sea (Fletcher et al., 2013) and a decrease in lake levels is also
513 observed in Central Europe (Magny et a., 2004) pointing to aridity during the DA. Evidences of
514 aridity during the DA have been show too in the Mediterranean part of the Iberian Peninsula, for
515 instance, cold and arid conditions were suggested in the northern Betic Range by the increase in

516   xerophytic herbs around 1450 and 750 cal yr BP (Carrión et al., 2001a) and in southeastern Spain
517   by a forest decline in lacustrine deposits around 1620 and 1160 cal yr BP (Carrión et al., 2003).
518   Arid and colder conditions during the Dark Ages (around 1680 to 1000 cal yr BP) are also
519   suggested for the central part of the Iberian Peninsula using a multiproxy study of a sediment
520   record from the Tablas de Daimiel Lake (Gil García et al., 2007).
521   A second period that we could differentiate within this overall arid phase occurred around 1100
522   to 600 cal yr BP/900 to 1350 CE, during the well-known MCA (900 to 1300 CE after Moreno et
523   al., 2012). During this period the Padul-15-05 record shows a slight increasing trend in the
524   Mediterranean forest taxa with respect to the DA, but the decrease in *Botryococcus* and the
525   higher abundance of herbs still point to overall arid conditions. This change could be related to
526   an increase in temperature, favoring the development of temperate forest species, and would
527   agree with inferred increasing temperatures in the North Atlantic areas, as well as the increase in
528   solar irradiance and the increase in SSTs in the Mediterranean Sea (Fig.7). This hypothesis
529   would agree with the reconstruction of persistent positive NAO and overall warm conditions
530   during the MCA in the western Mediterranean (see synthesis in Moreno et al., 2012). A similar
531   pattern of increasing xerophytic vegetation during the MCA is observed in alpine peat bogs and
532   lakes in the Sierra Nevada (Anderson et al., 2011; Jiménez-Moreno et al., 2013; Ramos-Román
533   et al., 2016) and arid conditions are shown to occur during the MCA in southern and eastern
534   Iberian Peninsula deduced by increases in salinity and lower lake levels (Corella et al., 2013;
535   Martín-Puertas et al., 2011). However, humid conditions have been reconstructed for the
536   northwestern of the Iberian Peninsula at this time (Lebreiro et al., 2006; Moreno et al., 2012), as
537   well as northern Europe (Martín-Puertas et al., 2008). The different pattern of precipitation
538   between the northwestern Iberian Peninsula / northern Europe and the Mediterranean area is
539   undoubtedly a function of the well-known NAO dipole in precipitation pattern (Trouet et al.,
540   2009).

5.2.4 The last ~600 cal yr BP: LIA (1350-1850 CE) and IE (1850 CE-Present)

542   Two climatically different periods can be distinguished during the last ca. 600 cal yr BP (end of
543   Zone 3b to Zone 4; Fig. 4) in the area. However, the climatic signal is more difficult to interpret
544   due to a higher human impact at that time. The first phase around 1350-1450 CE was
545   characterized by increasing relative humidity by the decrease in xerophytes and the increase in
546   Mediterranean forest taxa and *Botryococcus* after a period of decrease during the DA and MCA,
547   corresponding to the LIA. The second phase is characterized here by the decrease in the
548   Mediterranean forest around 1700-1850 CE, pointing to a return to more arid conditions during
549   the last part of the LIA (Figs. 4 and 7). This climatic pattern agrees with an increase in
550   precipitation by the transition from positive to negative NAO mode and from warmer to cooler
551   conditions in the North Atlantic area during the first phase of the LIA and a second phase
552   characterized by cooler (cold event 0; Bond et al., 2001) and drier conditions (Fig. 6). A stronger
553   variability in the SSTs is described in the Mediterranean Sea during the LIA (Fig. 6). Mayewski
554   et al. (2004) described a period of climate variability during the Holocene at this time (600 to
555   150 cal yr BP) suggesting a polar cooling but more humid in some parts of the tropics.
556   Regionally, (Morellón et al., 2011) also described a phase of more humid conditions between
557   1530 to 1750 CE in a lake sediment record from NE Spain. An alternation between wetter to
558   drier periods during the LIA are also shown in the nearby alpine record from Borreguil de la
559   Caldera in the Sierra Nevada mountain range (Ramos-Román et al., 2016).

560 The environmental transition from ephemeral to emerged conditions, observed in the last ca.
561 1550 cal yr BP (Unit 1; Fig. 5), intensified in the last ca. 300 cal yr BP. This is shown by the
562 highest MS and Si values the increase in wetland plants and the stronger decrease in Ca and
563 organic components (TOC) in the sediments in the uppermost part of the Padul-15-05 record
564 (Unit 2; Figs. 3 and 6).

565 **5.3 Centennial-scale variability**

566 Time series analysis has become important in determining the recurrent periodicity of cyclical
567 oscillations in paleoenvironmental sequences (e.g. Jiménez-Espejo et al., 2014; Ramos-Román et
568 al., 2016; Rodrigo-Gámiz et al., 2014; Fletcher et al., 2013). This analysis also assists in
569 understanding possible relationships between the paleoenvironmental proxy data and the
570 potential triggers of the observed cyclical changes: i.e., solar activity, atmospheric, oceanic
571 dynamics and climate evolution during the Holocene. The cyclostratigraphic analysis on the
572 pollen (Mediterranean forest; regional signal), algae (*Botryococcus*; local signal) and TOC (local
573 signal) times series from the Padul-15-05 record evidence centennial-scale cyclical patterns with
574 periodicities around 800, 680, 300, 240, 200 and 170 years above the 90 % confidence levels
575 (Fig. 7).
576 Previous cyclostratigraphic analysis in Holocene western Mediterranean records suggest cyclical
577 climatic oscillations with periodicities around 1500 and 1750 yr (Fletcher et al., 2013; Jiménez-
578 Espejo et al., 2014; Rodrigo-Gámiz et al., 2014). Other North Atlantic and Mediterranean
579 records also present cyclicities in their paleoclimatic proxies of ca. 1600 yr (Bond et al., 2001;
580 Debret et al., 2007; Rodrigo-Gámiz et al., 2014). However, this cycle is absent from the
581 cyclostratigraphic analysis in the Padul-15-05 record (Fig. 7). In contrast, the spectral analysis
582 performed in the Mediterranean forest time series from Padul peat bog record, pointing to
583 cyclical hydrological changes, shows a significant ~800 yr cycle that could be related to solar
584 variability (Damon and Sonett, 1991) or could be the second harmonic of the ca. ~1600 yr
585 oceanic-related cycle (Debret et al., 2009). A very similar periodicity of ca. 760 yr is detected in
586 the *Pinus* forest taxa, also pointing to humidity variability, from the alpine Sierra Nevada site of
587 Borreguil de la Caldera and seems to show that this is a common feature of cyclical
588 paleoclimatic oscillation in the area.
589 A significant ~680 cycle is shown in the *Botryococcus* time series most likely suggesting
590 recurrent centennial-scale changes in temperature (productivity) and water availability. A similar
591 cycle is shown in the *Artemisia* signal in an alpine record from Sierra Nevada (Ramos-Román et
592 al., 2016). This cycle around ~650 yr is also observed in a marine record from the Alboran Sea,
593 and was interpreted as the secondary harmonic of the 1300 yr cycle that those authors related
594 with cyclic thermohaline circulation and sea surface temperature changes (Rodrigo-Gámiz et al.,
595 2014).
596 A statistically significant ~300 yr cycle is shown in the Mediterranean forest taxa and TOC from
597 the Padul-15-05 record suggesting shorter-scale variability in water availability. This cycle is
598 also observed in the cyclical *Pinus* pollen data from Borreguil de la Caldera at higher elevations
599 in the Sierra Nevada (Ramos-Román et al., 2016). This cycle could be principally related to
600 NAO variability as observed by Olsen et al. (2012), which follows variations in humidity
601 observed in the Padul-15-05 record. NAO variability also regulates modern precipitation in the
602 area.
603 The *Botryococcus* and TOC time series shows variability with a periodicity around ~240, 200
604 and 164 yrs. Sonnet et al. (1984) described a significant cycle in solar activity around ~208 yr

605 (Suess solar cycle), which could have triggered our ~200 cyclicity. The observed ~240 yr
606 periodicity in the Padul-15-05 record could be either related to variations in solar activity or due
607 to the mixed effect of the solar together with the ~300 yr NAO-interpreted cycle and could point
608 to a solar origin of the centennial-scale NAO variations as suggested by previously published
609 research (Lukianova and Alekseev, 2004; Zanchettin et al., 2008). Finally, a significant ~170 yr
610 cycle has been observed in both the Mediterranean forest taxa and *Botryococcus* times series
611 from the Padul-15-05 record. A similar cycle (between 168-174 yr) was also described in the
612 alpine pollen record from Borreguil de la Caldera in Sierra Nevada (Ramos-Román et al., 2016),
613 which shows that it is a significant cyclical pattern in climate, probably precipitation, in the area.
614 This cycle could be related to the previously described ~170 yr cycle in the NAO index (Olsen et
615 al., 2012), which would agree with the hypothesis of the NAO controlling millennial- and
616 centennial-scale environmental variability during the Late Holocene in the area (García-Alix et
617 al., 2017; Ramos-Román et al., 2016).

618 **5.4 Human activity**

619 Humans probably had an impact in the area since Prehistoric times, however, the Padul-15-05
620 multiproxy record shows a more significant human impact during the last ca. 1550 cal yr BP,
621 which intensified in the last ca. 500 cal yr BP (since 1450 CE to Present). This is deduced by a
622 significant increase in nitrophilous plant taxa such as Cichorioideae, Convolvulaceae,
623 Polygonaceae and *Plantago* and the increase in some NPP such as *Tilletia*, coprophilous fungi
624 and thecamoebians (Unit 2; Pollen Zone 4; Fig. 4). Most of these pollen taxa and NPPs are
625 described in other southern Iberian paleoenvironmental records as indicators of land uses, for
626 instance, *Tilletia* and covarying Cichorioideae and Convolvulaceae have been described as
627 indicators of farming (e.g. Carrión et al., 2001b). Interestingly, these taxa being to decline around
628 ~1450 CE, coinciding with the higher increase in detritic material into the basin. Climatically,
629 this event coincides with the start of persistent negative NAO conditions in the area (Trouet et
630 al., 2009), which could have further triggered more rainfall and more detritic input into the basin.
631 Bellin et al., 2011 in a study from the Betic Cordillera (southern Iberian Peninsula) demonstrate
632 that soil erosion increase in years with higher rainfall and this could be intensified by human
633 impact. Nevertheless, in a study in the southeastern part of the Iberian Peninsula (Bellin et al.,
634 2013) suggested that major soil erosion could have occurred by the abandonment of agricultural
635 activities in the mountain areas as well as the abandonment of irrigated terrace systems during
636 the Christian Reconquest. Enhanced soil erosion at this time is also supported by the increase in
637 *Glomus* type (Fig. 4).
638 An important change in the sedimentation in the environment is observed during the last ca. 300
639 cal yr BP marked by the stronger increase in MS and Si values. This was probably related with
640 the Padul peat bog water drainage by humans using canals in the late XVIII century for
641 cultivation purposes (Villegas Molina, 1967). The increase in wetland vegetation and higher
642 values of Poaceae could be due to cultivation of cereals or by an increase in the population of
643 *Phragmites australis* (also a Poaceae), very abundant in the Padul peat bog margins at present
644 due to the increase in drained land surface.
645 The uppermost part (last ca. 100 cal yr BP) of the pollen record from Padul-15-05 shows an
646 increasing trend in some arboreal taxa at that time, including Mediterranean forest, *Olea* and
647 *Pinus* (Fig. 4). This change is most likely of human origin and generated by the increase in *Olea*
648 cultivation in the last two centuries, also observed in many records from higher elevation sites
649 from Sierra Nevada, and *Pinus* and other Mediterranean species reforestation in the 20th century

650   (Anderson et al., 2011; Jiménez-Moreno and Anderson, 2012; Jiménez-Moreno et al., 2013;
651   Ramos-Román et al., 2016).

6 Conclusions

653   Our multiproxy (i.e. lithology, geochemistry, paleontology) analysis from the Padul-15-05
654   sequence has provided a detailed climate reconstruction for the last 4700 ca yr BP for the Padul
655   peat bog area and the western Mediterranean. This study, supported by the comparison with
656   other Mediterranean and North Atlantic records suggests a link between vegetation, atmospheric
657   dynamics and insolation and solar activity during the Late Holocene in this area. A climatic
658   aridification trend occurred during the Late Holocene in the Sierra Nevada and the western
659   Mediterranean area, probably linked with the orbital-scale decreasing trend in summer
660   insolation. This long-term trend is modulated by centennial-scale climate variability as shown by
661   the pollen (Mediterranean forest taxa) algae (*Botryococcus*) and sedimentary and geochemical
662   data in the Padul record. These events are in correlation with regional and global scale climate
663   variability and cold and arid pulses around the 4200 and 3000 cal yr BP that are identified in this
664   study seem to be synchronous with cold events recorded in the North Atlantic and decreases in
665   precipitation in the Mediterranean area, probably linked to persistent positive NAO mode.
666   Moreover, one of the most important humid and warmer periods during the Late Holocene in the
667   Padul area coincides in time with the well-known IRHP, warm and humid conditions in the
668   Mediterranean and North Atlantic regions and overall negative NAO conditions. A drastic
669   decrease in Mediterranean forest taxa towards an open landscape, pointing to colder and
670   enhanced aridity, occurred in two steps (DA and end of the LIA) during the last ca. 1550 cal yr
671   BP. However, this trend was slightly superimposed by a more arid but warmer event coinciding
672   with the MCA and a cold but wetter event during the first part of the LIA. Besides natural
673   climatic and environmental variability, there seems to be intense human activities in the area
674   during the last the last ca. 1550 cal yr BP. This suggests that the natural aridification trend during
675   the Late Holocene in the western Mediterranean region could have been intensified due to the
676   higher human activity in this area.
677   Furthermore, time series analyses done in the Padul-15-05 record show centennial-scale changes
678   in the environment and climate that are coincident with the periodicities observed in solar,
679   oceanic and NAO reconstructions and could show a close cause-and-effect linkage between
680   them.

Acknowledgement

682   This work was supported by the project P11-RNM-7332 funded by Consejería de Economía,
683   Innovación, Ciencia y Empleo de la Junta de Andalucía, the project CGL2013-47038-R funded
684   by Ministerio de Economía y Competitividad of Spain and fondo Europeo de desarrollo regional
685   FEDER and the research group RNM0190 (Junta de Andalucía). M. J. R.-R. acknowledges the
686   PhD funding provided by Consejería de Economía, Innovación, Ciencia y Empleo de la Junta de
687   Andalucía (P11-RNM-7332). J.C. acknowledges the PhD funding provided by Ministerio de
688   Economía y Competitividad (CGL2013-47038-R). A.G.-A. was also supported by a Ramón y
689   Cajal Fellowship RYC-2015-18966 of the Spanish Government (Ministerio de Economía y
690   Competitividad). Javier Jaimez (CIC-UGR) is thanked for graciously helping with the coring, the
691   drilling equipment and logistics.

692   **References**

693   Abel-Schaad, D. and López-Sáez, J. A.: Vegetation changes in relation to fire history and human
694   activities at the Peña Negra mire (Bejar Range, Iberian Central Mountain System, Spain) during
695   the past 4,000 years, Veg. Hist. Archaeobotany, 22(3), 199–214, doi:10.1007/s00334-012-0368-
696   9, 2013.

697   Al Aallali, A., Nieto, J. M. L., Raya, F. A. P. and Mesa, J. M.: Estudio de la vegetación forestal en la
698   vertiente sur de Sierra Nevada (Alpujarra Alta granadina), Itinera Geobot., (11), 387–402, 1998.

699   Alfaro, P., Galinod-Zaldievar, J., Jabaloy, A., López-Garrido, A. C. and Sanz de Galdeano, C.:
700   Evidence for the activity and paleoseismicity of the Padul fault (Betic Cordillera, Southern Spain)
701   [Evidencias de actividad y paleosismicidad de la falla de Padul (Cordillera Bética, sur de
702   España)], Acta Geol. Hisp., 36(3–4), 283–297, 2001.

703   Alpert, P., Baldi, M., Ilani, R., Krichak, S., Price, C., Rodó, X., Saaroni, H., Ziv, B., Kishcha, P.,
704   Barkan, J., Mariotti, A. and Xoplaki, E.: Chapter 2 Relations between climate variability in the
705   Mediterranean region and the tropics: ENSO, South Asian and African monsoons, hurricanes
706   and Saharan dust, Dev. Earth Environ. Sci., 4(C), 149–177, doi:10.1016/S1571-9197(06)80005-4,
707   2006.

708   Anderson, R. S., Jiménez-Moreno, G., Carrión, J. S. and Pérez-Martínez, C.: Postglacial history of
709   alpine vegetation, fire, and climate from Laguna de Río Seco, Sierra Nevada, southern Spain,
710   Quat. Sci. Rev., 30(13–14), 1615–1629, doi:https://doi.org/10.1016/j.quascirev.2011.03.005,
711   2011.

712   Bar-Matthews, M., Ayalon, A., Gilmour, M., Matthews, A. and Hawkesworth, C. J.: Sea–land
713   oxygen isotopic relationships from planktonic foraminifera and speleothems in the Eastern
714   Mediterranean region and their implication for paleorainfall during interglacial intervals,
715   Geochim. Cosmochim. Acta, 67(17), 3181–3199, doi:https://doi.org/10.1016/S0016-
716   7037(02)01031-1, 2003.

717   Bellin, N., Vanacker, V., van Wesemael, B., Solé-Benet, A. and Bakker, M. M.: Natural and
718   anthropogenic controls on soil erosion in the internal betic Cordillera (southeast Spain), Catena,
719   87(2), 190–200, doi:10.1016/j.catena.2011.05.022, 2011.

720   Bellin, N., Vanacker, V. and De Baets, S.: Anthropogenic and climatic impact on Holocene
721   sediment dynamics in SE Spain: A review, Quat. Int., 308–309, 112–129,
722   doi:10.1016/j.quaint.2013.03.015, 2013.

723   Beug, H.-J.: Leitfaden der Pollenbestimmung für Mitteleuropa und angrenzende Gebiete, Fisch.
724   Stuttg., 61, 1961.

725   Blaauw, M.: Methods and code for "classical" age-modelling of radiocarbon sequences, Quat.
726   Geochronol., 5(5), 512–518, doi:https://doi.org/10.1016/j.quageo.2010.01.002, 2010.

727 Bond, G., Kromer, B., Beer, J., Muscheler, R., Evans, M. N., Showers, W., Hoffmann, S., Lotti-
728 Bond, R., Hajdas, I. and Bonani, G.: Persistent Solar Influence on North Atlantic Climate During
729 the Holocene, Science, 294(5549), 2130, doi:10.1126/science.1065680, 2001.

730 Booth, R. K., Jackson, S. T., Forman, S. L., Kutzbach, J. E., E. A. Bettis, I., Kreigs, J. and Wright, D.
731 K.: A severe centennial-scale drought in midcontinental North America 4200 years ago and
732 apparent global linkages, The Holocene, 15(3), 321–328, doi:10.1191/0959683605hl825ft,
733 2005.

734 Carrión, J. S.: Patterns and processes of Late Quaternary environmental change in a montane
735 region of southwestern Europe, Quat. Sci. Rev., 21(18–19), 2047–2066,
736 doi:https://doi.org/10.1016/S0277-3791(02)00010-0, 2002.

737 Carrión, J. S., Munuera, M., Dupré, M. and Andrade, A.: Abrupt vegetation changes in the
738 Segura Mountains of southern Spain throughout the Holocene, J. Ecol., 89(5), 783–797,
739 doi:10.1046/j.0022-0477.2001.00601.x, 2001a.

740 Carrión, J. S., Andrade, A., Bennett, K. D., Navarro, C. and Munuera, M.: Crossing forest
741 thresholds: inertia and collapse in a Holocene sequence from south-central Spain, The
742 Holocene, 11(6), 635–653, doi:10.1191/09596830195672, 2001b.

743 Carrión, J. S., Fernández, S., Jiménez-Moreno, G., Fauquette, S., Gil-Romera, G., González-
744 Sampériz, P. and Finlayson, C.: The historical origins of aridity and vegetation degradation in
745 southeastern Spain, J. Arid Environ., 74(7), 731–736,
746 doi:https://doi.org/10.1016/j.jaridenv.2008.11.014, 2010b.

747 Carrión, J. S., Sánchez-Gómez, P., Mota, J. F., Yll, R. and Chaín, C.: Holocene vegetation
748 dynamics, fire and grazing in the Sierra de Gádor, southern Spain, Holocene, 13(6), 839–849,
749 doi:10.1191/0959683603hl662rp, 2003.

750 Carrión, J. S., Fuentes, N., González-Sampériz, P., Quirante, L. S., Finlayson, J. C., Fernández, S.
751 and Andrade, A.: Holocene environmental change in a montane region of southern Europe with
752 a long history of human settlement, Quat. Sci. Rev., 26(11–12), 1455–1475,
753 doi:https://doi.org/10.1016/j.quascirev.2007.03.013, 2007.

754 Carrión, J. S., Fernández, S., González-Sampériz, P., Gil-Romera, G., Badal, E., Carrión-Marco, Y.,
755 López-Merino, L., López-Sáez, J. A., Fierro, E. and Burjachs, F.: Expected trends and surprises in
756 the Lateglacial and Holocene vegetation history of the Iberian Peninsula and Balearic Islands,
757 Rev. Palaeobot. Palynol., 162(3), 458–475,
758 doi:http://dx.doi.org/10.1016/j.revpalbo.2009.12.007, 2010.

759 Combourieu-Nebout, N., Peyron, O., Dormoy, I., Desprat, S., Beaudouin, C., Kotthoff, U. and
760 Marret, F.: Rapid climatic variability in the west Mediterranean during the last 25 000 years
761 from high resolution pollen data, Clim Past, 5(3), 503–521, doi:10.5194/cp-5-503-2009, 2009.

762 Corella, J. P., Stefanova, V., El Anjoumi, A., Rico, E., Giralt, S., Moreno, A., Plata-Montero, A. and

763   Valero-Garcés, B. L.: A 2500-year multi-proxy reconstruction of climate change and human
764   activities in northern Spain: The Lake Arreo record, Palaeogeogr. Palaeoclimatol. Palaeoecol.,
765   386, 555–568, doi:10.1016/j.palaeo.2013.06.022, 2013.

766   Currás, A., Zamora, L., Reed, J. M., García-Soto, E., Ferrero, S., Armengol, X., Mezquita-Joanes,
767   F., Marqués, M. A., Riera, S. and Julià, R.: Climate change and human impact in central Spain
768   during Roman times: High-resolution multi-proxy analysis of a tufa lake record (Somolinos,
769   1280m asl), Catena, 89(1), 31–53, doi:10.1016/j.catena.2011.09.009, 2012.

770   Damon, P. E. and Sonett, C. P.: Solar and terrestrial components of the atmospheric C-14
771   variation spectrum. In: Sonett, C.P., Giampapa, M.S., Matthews, M.S. (Eds.), The Sun in Time.
772   University of Arizona Press, Tucson, AZ, USA., 1991.

773   Debret, M., Bout-Roumazeilles, V., Grousset, F., Desmet, M., McManus, J. F., Massei, N., Sebag,
774   D., Petit, J.-R., Copard, Y. and Trentesaux, A.: The origin of the 1500-year climate cycles in
775   holocene north-atlantic records, Clim. Past, 3(4), 569–575, 2007.

776   Debret, M., Sebag, D., Crosta, X., Massei, N., Petit, J.-R., Chapron, E. and Bout-Roumazeilles, V.:
777   Evidence from wavelet analysis for a mid-Holocene transition in global climate forcing, Quat.
778   Sci. Rev., 28(25–26), 2675–2688, doi:https://doi.org/10.1016/j.quascirev.2009.06.005, 2009.

779   Delgado, J., Alfaro, P., Galindo-Zaldivar, J., Jabaloy, A., Lopez Garrido, A. and Sanz de Galdeano,
780   C.: Structure of the Padul-Nigüelas basin (S Spain) from H/V ratios of ambient noise: application
781   of the method to study peat and coarse sediments, Pure Appl. Geophys., 159(11), 2733–2749,
782   2002.

783   Domingo-García, M., Fernández-Rubio, R., Lopez, J. and González, C.: Aportación al
784   conocimiento de la Neotectónica de la Depresión del Padul (Granada), Tecniterrae, 53, 6–16,
785   1983.

786   Ejarque, A., Anderson, R. S., Simms, A. R. and Gentry, B. J.: Prehistoric fires and the shaping of
787   colonial transported landscapes in southern California: A paleoenvironmental study at Dune
788   Pond, Santa Barbara County, Quat. Sci. Rev., 112, 181–196,
789   doi:https://doi.org/10.1016/j.quascirev.2015.01.017, 2015.

790   Faegri, K. and Iversen, J.: Textbook of Pollen Analysis. Wiley, New York., 1989.

791   Fletcher, W. J. and Sánchez-Goñi, M. F.: Orbital- and sub-orbital-scale climate impacts on
792   vegetation of the western Mediterranean basin over the last 48,000 yr, Quat. Res., 70(3), 451–
793   464, doi:10.1016/j.yqres.2008.07.002, 2008.

794   Fletcher, W. J., Debret, M. and Sánchez-Goñi, M. F.: Mid-Holocene emergence of a low-
795   frequency millennial oscillation in western Mediterranean climate: Implications for past
796   dynamics of the North Atlantic atmospheric westerlies, The Holocene, 23(2), 153–166,
797   doi:10.1177/0959683612460783, 2013.

798 Florschütz, F., Amor, J. M. and Wijmstra, T. A.: Palynology of a thick quaternary succession in
799 southern Spain, Palaeogeogr. Palaeoclimatol. Palaeoecol., 10(4), 233–264,
800 doi:http://dx.doi.org/10.1016/0031-0182(71)90049-6, 1971.

801 García-Alix, A., Jimenez-Espejo, F. J., Lozano, J. A., Jiménez-Moreno, G., Martinez-Ruiz, F.,
802 Sanjuán, L. G., Jiménez, G. A., Alfonso, E. G., Ruiz-Puertas, G. and Anderson, R. S.:
803 Anthropogenic impact and lead pollution throughout the Holocene in Southern Iberia, Sci. Total
804 Environ., 449, 451–460, doi:https://doi.org/10.1016/j.scitotenv.2013.01.081, 2013.

805 García-Alix, A., Jiménez-Espejo, F. J., Toney, J. L., Jiménez-Moreno, G., Ramos-Román, M. J.,
806 Anderson, R. S., Ruano, P., Queralt, I., Delgado Huertas, A. and Kuroda, J.: Alpine bogs of
807 southern Spain show human-induced environmental change superimposed on long-term
808 natural variations, Sci. Rep., 7(1), 7439, doi:10.1038/s41598-017-07854-w, 2017.

809 van Geel, B., Hallewas, D. P. and Pals, J. P.: A late holocene deposit under the Westfriese Zeedijk
810 near Enkhuizen (Prov. of Noord-Holland, The Netherlands): Palaeoecological and archaeological
811 aspects, Rev. Palaeobot. Palynol., 38(3), 269–335, doi:http://dx.doi.org/10.1016/0034-
812 6667(83)90026-X, 1983.

813 van Geel, B., Coope, G. R. and Hammen, T. V. D.: Palaeoecology and stratigraphy of the
814 lateglacial type section at Usselo (the Netherlands), Rev. Palaeobot. Palynol., 60(1), 25–129,
815 doi:http://dx.doi.org/10.1016/0034-6667(89)90072-9, 1989.

816 Gil García, M. J., Ruiz Zapata, M. B., Santisteban, J. I., Mediavilla, R., López-Pamo, E. and Dabrio,
817 C. J.: Late holocene environments in Las Tablas de Daimiel (south central Iberian peninsula,
818 Spain), Veg. Hist. Archaeobotany, 16(4), 241–250, doi:10.1007/s00334-006-0047-9, 2007.

819 Gil-Romera, G., González-Sampériz, P., Lasheras-Álvarez, L., Sevilla-Callejo, M., Moreno, A.,
820 Valero-Garcés, B., López-Merino, L., Carrión, J. S., Pérez Sanz, A., Aranbarri, J. and García-Prieto
821 Fronce, E.: Biomass-modulated fire dynamics during the Last Glacial–Interglacial Transition at
822 the Central Pyrenees (Spain), Palaeogeogr. Palaeoclimatol. Palaeoecol., 402, 113–124,
823 doi:https://doi.org/10.1016/j.palaeo.2014.03.015, 2014.

824 Grimm, E. C.: CONISS: a FORTRAN 77 program for stratigraphically constrained cluster analysis
825 by the method of incremental sum of squares, Comput. Geosci., 13(1), 13–35,
826 doi:http://dx.doi.org/10.1016/0098-3004(87)90022-7, 1987.

827 Guy-Ohlson, D.: Botryococcus as an aid in the interpretation of palaeoenvironment and
828 depositional processes, Rev. Palaeobot. Palynol., 71(1), 1–15,
829 doi:http://dx.doi.org/10.1016/0034-6667(92)90155-A, 1992.

830 Hurrell, J. W.: Decadal Trends in the North Atlantic Oscillation: Regional Temperatures and
831 Precipitation, Science, 269(5224), 676, doi:10.1126/science.269.5224.676, 1995.

832 Jalut, G., Dedoubat, J. J., Fontugne, M. and Otto, T.: Holocene circum-Mediterranean vegetation
833 changes: Climate forcing and human impact, Quat. Int., 200(1–2), 4–18,

834   doi:https://doi.org/10.1016/j.quaint.2008.03.012, 2009.

835   Jiménez-Espejo, F. J., García-Alix, A., Jiménez-Moreno, G., Rodrigo-Gámiz, M., Anderson, R. S.,
836   Rodríguez-Tovar, F. J., Martínez-Ruiz, F., Giralt, S., Delgado Huertas, A. and Pardo-Igúzquiza, E.:
837   Saharan aeolian input and effective humidity variations over western Europe during the
838   Holocene from a high altitude record, Chem. Geol., 374–375, 1–12,
839   doi:10.1016/j.chemgeo.2014.03.001, 2014.

840   Jiménez-Moreno, G. and Anderson, R. S.: Holocene vegetation and climate change recorded in
841   alpine bog sediments from the Borreguiles de la Virgen, Sierra Nevada, southern Spain, Quat.
842   Res., 77(1), 44–53, doi:10.1016/j.yqres.2011.09.006, 2012.

843   Jiménez-Moreno, G., García-Alix, A., Hernández-Corbalán, M. D., Anderson, R. S. and Delgado-
844   Huertas, A.: Vegetation, fire, climate and human disturbance history in the southwestern
845   Mediterranean area during the late Holocene, Quat. Res., 79(2), 110–122,
846   doi:https://doi.org/10.1016/j.yqres.2012.11.008, 2013.

847   Jiménez-Moreno, G., Rodríguez-Ramírez, A., Pérez-Asensio, J. N., Carrión, J. S., López-Sáez, J. A.,
848   Villarías-Robles, J. J. R., Celestino-Pérez, S., Cerrillo-Cuenca, E., León, Á. and Contreras, C.:
849   Impact of late-Holocene aridification trend, climate variability and geodynamic control on the
850   environment from a coastal area in SW Spain, Holocene, 25(4), 607–617,
851   doi:10.1177/0959683614565955, 2015.

852   Kalugin, I., Daryin, A., Smolyaninova, L., Andreev, A., Diekmann, B. and Khlystov, O.: 800-yr-long
853   records of annual air temperature and precipitation over southern Siberia inferred from
854   Teletskoye Lake sediments, Quat. Res., 67(3), 400–410,
855   doi:https://doi.org/10.1016/j.yqres.2007.01.007, 2007.

856   Laskar, J., Robutel, P., Joutel, F., Gastineau, M., Correia, A. C. M. and Levrard, B.: A long-term
857   numerical solution for the insolation quantities of the Earth, A&A, 428(1), 261–285,
858   doi:10.1051/0004-6361:20041335, 2004.

859   Lebreiro, S. M., Francés, G., Abrantes, F. F. G., Diz, P., Bartels-Jónsdóttir, H. B., Stroynowski, Z.
860   N., Gil, I. M., Pena, L. D., Rodrigues, T., Jones, P. D., Nombela, M. A., Alejo, I., Briffa, K. R., Harris,
861   I. and Grimalt, J. O.: Climate change and coastal hydrographic response along the Atlantic
862   Iberian margin (Tagus Prodelta and Muros Ría) during the last two millennia, Holocene, 16(7),
863   1003–1015, doi:10.1177/0959683606hl990rp, 2006.

864   Lillios, K. T., Blanco-González, A., Drake, B. L. and López-Sáez, J. A.: Mid-late Holocene climate,
865   demography, and cultural dynamics in Iberia: A multi-proxy approach, Quat. Sci. Rev., 135, 138–
866   153, doi:https://doi.org/10.1016/j.quascirev.2016.01.011, 2016.

867   López-Sáez, J. A., Abel-Schaad, D., Pérez-Díaz, S., Blanco-González, A., Alba-Sánchez, F., Dorado,
868   M., Ruiz-Zapata, B., Gil-García, M. J., Gómez-González, C. and Franco-Múgica, F.: Vegetation
869   history, climate and human impact in the Spanish Central System over the last 9000 years,

870   Quat. Int., 353, 98–122, doi:https://doi.org/10.1016/j.quaint.2013.06.034, 2014.

871   Lukianova, R. and Alekseev, G.: Long-Term Correlation Between the Nao and Solar Activity, Sol.
872   Phys., 224(1), 445–454, doi:10.1007/s11207-005-4974-x, 2004.

873   Magny, M.: Holocene climate variability as reflected by mid-European lake-level fluctuations
874   and its probable impact on prehistoric human settlements, Quat. Int., 113(1), 65–79,
875   doi:https://doi.org/10.1016/S1040-6182(03)00080-6, 2004.

876   Magny, M., Peyron, O., Sadori, L., Ortu, E., Zanchetta, G., Vannière, B. and Tinner, W.:
877   Contrasting patterns of precipitation seasonality during the Holocene in the south- and north-
878   central Mediterranean, J. Quat. Sci., 27(3), 290–296, doi:10.1002/jqs.1543, 2012.

879   Magri, D.: Late Quaternary vegetation history at Lagaccione near Lago di Bolsena (central Italy),
880   Rev. Palaeobot. Palynol., 106(3–4), 171–208, doi:https://doi.org/10.1016/S0034-
881   6667(99)00006-8, 1999.

882   Marchal, O., Cacho, I., Stocker, T. F., Grimalt, J. O., Calvo, E., Martrat, B., Shackleton, N.,
883   Vautravers, M., Cortijo, E., Van Kreveld, S., Andersson, C., Koç, N., Chapman, M., Sbaffi, L.,
884   Duplessy, J.-C., Sarnthein, M., Turon, J.-L., Duprat, J. and Jansen, E.: Apparent long-term cooling
885   of the sea surface in the northeast Atlantic and Mediterranean during the Holocene, Quat. Sci.
886   Rev., 21(4–6), 455–483, doi:10.1016/S0277-3791(01)00105-6, 2002.

887   Martín-Puertas, C., Valero-Garcés, B. L., Mata, M. P., González-Sampériz, P., Bao, R., Moreno, A.
888   and Stefanova, V.: Arid and humid phases in southern Spain during the last 4000 years: the
889   Zoñar Lake record, Córdoba, The Holocene, 18(6), 907–921, doi:10.1177/0959683608093533,
890   2008.

891   Martín-Puertas, C., Valero-Garcés, B. L., Brauer, A., Mata, M. P., Delgado-Huertas, A. and Dulski,
892   P.: The Iberian-Roman Humid Period (2600-1600 cal yr BP) in the Zoñar Lake varve record
893   (Andalucía, southern Spain), Quat. Res., 71(2), 108–120, doi:10.1016/j.yqres.2008.10.004, 2009.

894   Martín-Puertas, C., Valero-Garcés, B. L., Mata, M. P., Moreno, A., Giralt, S., Martínez-Ruiz, F.
895   and Jiménez-Espejo, F.: Geochemical processes in a Mediterranean Lake: A high-resolution
896   study of the last 4,000 years in Zoñar Lake, southern Spain, J. Paleolimnol., 46(3), 405–421,
897   doi:10.1007/s10933-009-9373-0, 2011.

898   Mayewski, P. A., Rohling, E. E., Stager, J. C., Karlén, W., Maasch, K. A., Meeker, L. D., Meyerson,
899   E. A., Gasse, F., Kreveld, S. van, Holmgren, K., Lee-Thorp, J., Rosqvist, G., Rack, F., Staubwasser,
900   M., Schneider, R. R. and Steig, E. J.: Holocene climate variability, Quat. Res., 62(3), 243–255,
901   doi:https://doi.org/10.1016/j.yqres.2004.07.001, 2004.

902   Morellón, M., Valero-Garcés, B., Vegas-Vilarrúbia, T., González-Sampériz, P., Romero, Ó.,
903   Delgado-Huertas, A., Mata, P., Moreno, A., Rico, M. and Corella, J. P.: Lateglacial and Holocene
904   palaeohydrology in the western Mediterranean region: The Lake Estanya record (NE Spain),
905   Quat. Sci. Rev., 28(25–26), 2582–2599, doi:https://doi.org/10.1016/j.quascirev.2009.05.014,

906   2009.

907   Morellón, M., Valero-Garcés, B., González-Sampériz, P., Vegas-Vilarrúbia, T., Rubio, E.,
908   Rieradevall, M., Delgado-Huertas, A., Mata, P., Romero, Ó., Engstrom, D. R., López-Vicente, M.,
909   Navas, A. and Soto, J.: Climate changes and human activities recorded in the sediments of Lake
910   Estanya (NE Spain) during the Medieval Warm Period and Little Ice Age, J. Paleolimnol., 46(3),
911   423–452, doi:10.1007/s10933-009-9346-3, 2011.

912   Moreno, A., Cacho, I., Canals, M., Grimalt, J. O., Sánchez-Goñi, M. F., Shackleton, N. and Sierro,
913   F. J.: Links between marine and atmospheric processes oscillating on a millennial time-scale. A
914   multi-proxy study of the last 50,000 yr from the Alboran Sea (Western Mediterranean Sea),
915   Quat. Sci. Rev., 24(14–15), 1623–1636, doi:https://doi.org/10.1016/j.quascirev.2004.06.018,
916   2005.

917   Moreno, A., Pérez, A., Frigola, J., Nieto-Moreno, V., Rodrigo-Gámiz, M., Martrat, B., González-
918   Sampériz, P., Morellón, M., Martín-Puertas, C., Corella, J. P., Belmonte, Á., Sancho, C., Cacho, I.,
919   Herrera, G., Canals, M., Grimalt, J. O., Jiménez-Espejo, F., Martínez-Ruiz, F., Vegas-Vilarrúbia, T.
920   and Valero-Garcés, B. L.: The Medieval Climate Anomaly in the Iberian Peninsula reconstructed
921   from marine and lake records, Quat. Sci. Rev., 43, 16–32,
922   doi:https://doi.org/10.1016/j.quascirev.2012.04.007, 2012.

923   Nestares, T. and Torres, T. de: Un nuevo sondeo de investigación paleoambiental del
924   Pleistoceno y Holoceno en la turbera del Padul (Granada, Andalucía). Geogaceta 23, 99-102.,
925   1997.

926   Olsen, J., Anderson, N. J. and Knudsen, M. F.: Variability of the North Atlantic Oscillation over
927   the past 5,200 years, Nat. Geosci, 5(11), 808–812, doi:10.1038/ngeo1589, 2012.

928   Ortiz, J. E., Torres, T., Delgado, A., Julià, R., Lucini, M., Llamas, F. J., Reyes, E., Soler, V. and Valle,
929   M.: The palaeoenvironmental and palaeohydrological evolution of Padul Peat Bog (Granada,
930   Spain) over one million years, from elemental, isotopic and molecular organic geochemical
931   proxies, Org. Geochem., 35(11–12), 1243–1260,
932   doi:https://doi.org/10.1016/j.orggeochem.2004.05.013, 2004.

933   Paillard, D., Labeyrie, L. and Yiou, P.: Macintosh Program performs time-series analysis, Eos
934   Trans. Am. Geophys. Union, 77(39), 379–379, doi:10.1029/96EO00259, 1996.

935   Pérez Raya, F. and López Nieto, J.: Vegetación acuática y helofítica de la depresión de Padul
936   (Granada), Acta Bot Malacit., 16(2), 373–389, 1991.

937   Pons, A. and Reille, M.: The holocene- and upper pleistocene pollen record from Padul
938   (Granada, Spain): A new study, Palaeogeogr. Palaeoclimatol. Palaeoecol., 66(3), 243–263,
939   doi:http://dx.doi.org/10.1016/0031-0182(88)90202-7, 1988.

940   Ramos-Román, M. J., Jiménez-Moreno, G., Anderson, R. S., García-Alix, A., Toney, J. L., Jiménez-
941   Espejo, F. J. and Carrión, J. S.: Centennial-scale vegetation and North Atlantic Oscillation

942   changes during the Late Holocene in the southern Iberia, Quat. Sci. Rev., 143, 84–95,
943   doi:https://doi.org/10.1016/j.quascirev.2016.05.007, 2016.

944   Reimer, P. J., Bard, E., Bayliss, A., Beck, J. W., Blackwell, P. G., Ramsey, C. B., Buck, C. E., Cheng,
945   H., Edwards, R. L., Friedrich, M., Grootes, P. M., Guilderson, T. P., Haflidason, H., Hajdas, I.,
946   Hatté, C., Heaton, T. J., Hoffmann, D. L., Hogg, A. G., Hughen, K. A., Kaiser, K. F., Kromer, B.,
947   Manning, S. W., Niu, M., Reimer, R. W., Richards, D. A., Scott, E. M., Southon, J. R., Staff, R. A.,
948   Turney, C. S. M. and van der Plicht, J.: IntCal13 and Marine13 Radiocarbon Age Calibration
949   Curves 0–50,000 Years cal BP, Radiocarbon, 55(4), 1869–1887, doi:10.2458/azu_js_rc.55.16947,
950   2013.

951   Riera, S., Wansard, G. and Julià, R.: 2000-year environmental history of a karstic lake in the
952   Mediterranean Pre-Pyrenees: the Estanya lakes (Spain), {CATENA}, 55(3), 293–324,
953   doi:https://doi.org/10.1016/S0341-8162(03)00107-3, 2004.

954   Riera, S., López-Sáez, J. A. and Julià, R.: Lake responses to historical land use changes in
955   northern Spain: The contribution of non-pollen palynomorphs in a multiproxy study, Rev.
956   Palaeobot. Palynol., 141(1–2), 127–137, doi:https://doi.org/10.1016/j.revpalbo.2006.03.014,
957   2006.

958   Rodrigo-Gámiz, M., Martínez-Ruiz, F., Rodríguez-Tovar, F. J., Jiménez-Espejo, F. J. and Pardo-
959   Igúzquiza, E.: Millennial- to centennial-scale climate periodicities and forcing mechanisms in the
960   westernmost Mediterranean for the past 20,000 yr, Quat. Res., 81(1), 78–93,
961   doi:https://doi.org/10.1016/j.yqres.2013.10.009, 2014.

962   Sanz de Galdeano, C., El Hamdouni, R. and Chacón, J.: Neotectónica de la fosa del Padul y del
963   Valle de Lecrín, Itiner. Geomorfológicos Por Andal. Orient. Publicacions Univ. Barc. Barc., 65–81,
964   1998.

965   Schulz, M. and Mudelsee, M.: REDFIT: estimating red-noise spectra directly from unevenly
966   spaced paleoclimatic time series, Comput. Geosci., 28(3), 421–426,
967   doi:https://doi.org/10.1016/S0098-3004(01)00044-9, 2002.

968   Sicre, M.-A., Jalali, B., Martrat, B., Schmidt, S., Bassetti, M.-A. and Kallel, N.: Sea surface
969   temperature variability in the North Western Mediterranean Sea (Gulf of Lion) during the
970   Common Era, Earth Planet. Sci. Lett., 456, 124–133,
971   doi:http://dx.doi.org/10.1016/j.epsl.2016.09.032, 2016.

972   Steinhilber, F., Beer, J. and Fröhlich, C.: Total solar irradiance during the Holocene, Geophys.
973   Res. Lett., 36(19), n/a–n/a, doi:10.1029/2009GL040142, 2009.

974   Trouet, V., Esper, J., Graham, N. E., Baker, A., Scourse, J. D. and Frank, D. C.: Persistent Positive
975   North Atlantic Oscillation Mode Dominated the Medieval Climate Anomaly, Science, 324(5923),
976   78, doi:10.1126/science.1166349, 2009.

977   Valle, F.: Mapa de series de vegetación de Andalucía 1: 400 000, Editorial Rueda., 2003.

978 Villegas Molina, F.: Laguna de Padul: Evolución geológico-histórica, Estud. Geográficos, 28(109),
979 561, 1967.

980 Zanchettin, D., Rubino, A., Traverso, P. and Tomasino, M.: Impact of variations in solar activity
981 on hydrological decadal patterns in northern Italy, J. Geophys. Res. Atmospheres, 113(D12),
982 n/a–n/a, doi:10.1029/2007JD009157, 2008.

983
984

985

986

987

988

989

990

991

992

993

994

995

996

997

998

999

1000

1001

1002

1003

1004

1005   **Figures and tables**
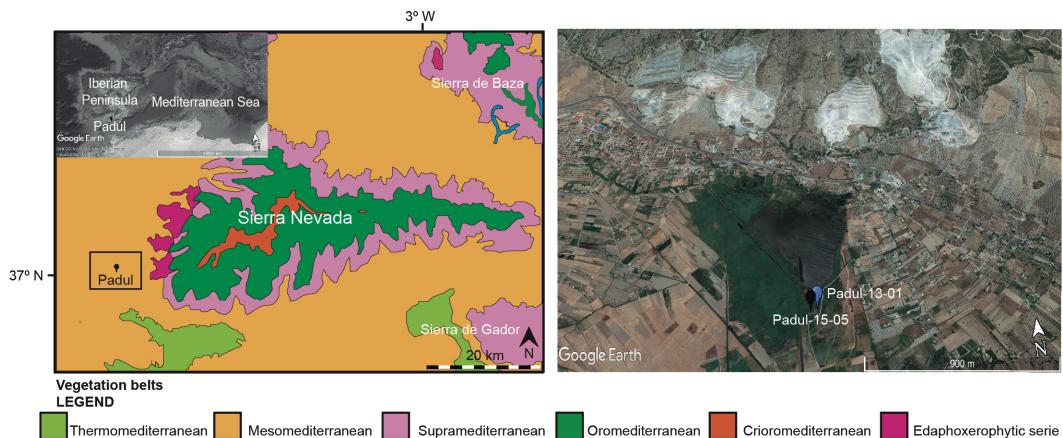
1006

1007   **Figure 1.** Location of Padul peat bog in Sierra Nevada National Park, southern Iberian
1008   Peninsula. Panel on the left is the map of the vegetation belts in the Sierra Nevada (Modified
1009   from   REDIAM.   Map   of   the   vegetation   series   of   Andalusia:
1010   http://laboratoriorediam.cica.es/VisorGenerico/?tipo=WMS&url=http://www.juntadeandalucia.e
1011   s/medioambiente/mapwms/REDIAM_Series_Vegetacion_Andalucia?). The inset map is the
1012   Google earth image of the Iberian Peninsula in the Mediterranean region. Panel on the right is
1013   the Google earth image (http://www.google.com/earth/index.html) of Padul peat bog area
1014   showing the coring locations.

1015

1016
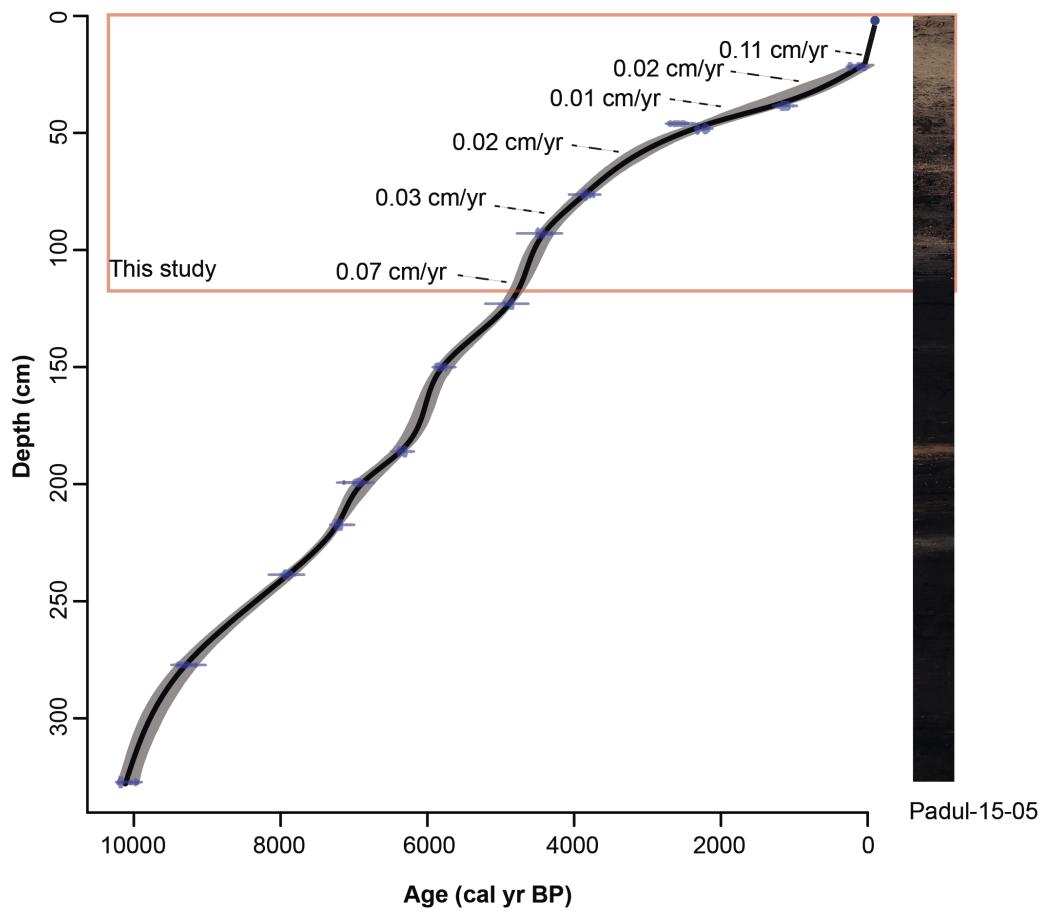
Figure 2. Photo of the Padul-15-05 sediment core with the age-depth model showing the part of the record that was studied here (red rectangle). The sediment accumulation rates (SAR) between individual segments are marked. See the body of the text for the explanation of the age reconstructions.
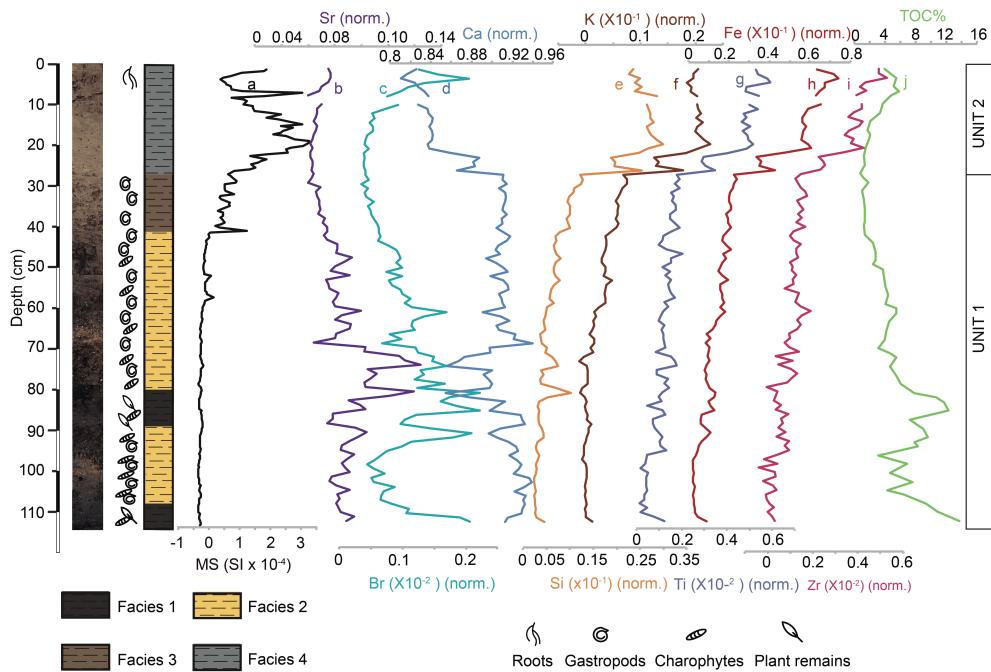
Figure 3. Lithology, facies interpretation with paleontology, magnetic susceptibility (MS), and geochemical (X-ray fluorescence (XRF) and total organic carbon (TOC) data from the Padul-15-05 record. XRF elements are represented normalized by the total counts. (a) Magnetic susceptibility (MS; SI). (b) Strontium normalized (Sr; norm.). (c) Bromine norm. (Br; norm.). (d) Calcium normalized. (Ca; norm.). (e) Silica normalized (Si; norm.). (f) Potassium normalized (K; norm.). (g) Titanium normalized (Ti; norm.). (h) Iron normalized (Fe; norm.). (i) Zirconium normalized (Zr; norm.). (j) Total organic carbon (TOC %).

1040
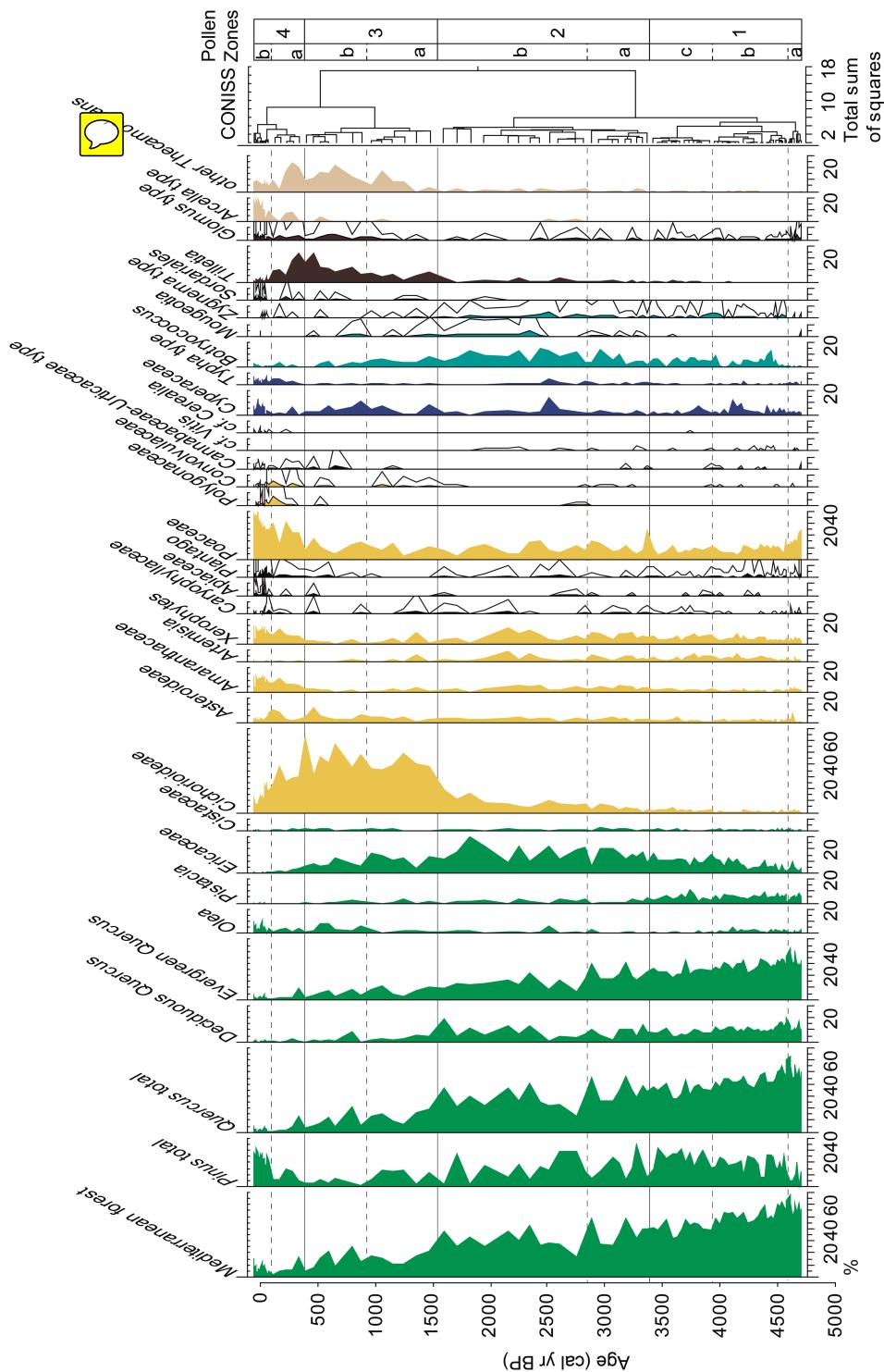
Figure 4. Percentages of selected pollen taxa and non-pollen palynomorphs (NPPs) from the Padul-15-05 record, represented with respect to terrestrial pollen sum. Silhouettes show 7-time exaggerations of pollen percentages. Pollen zonation is shown on the right. Tree and shrubs are showing in green, herbs and grasses in yellow, aquatics in dark blue, algae in blue, fungi in brown and thecamoebians in beige. The Mediterranean forest taxa is composed of *Quercus* total, *Olea*, *Phillyrea* and *Pistacia*. The xerophyte group includes *Artemisia*, *Ephedra*, and Amaranthaceae.
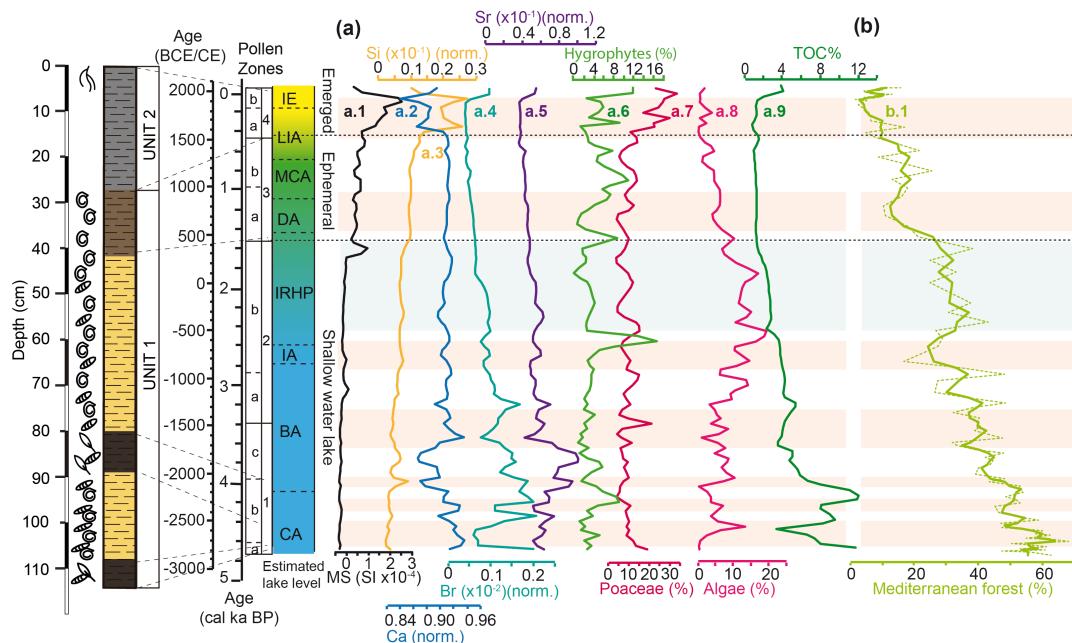
Figure 5. Estimated lake level evolution and regional palynological component from the last ca. 4700 yr based on the synthesis of determinate proxies from the Padul-15-05 record: (a) Proxies used to estimate the water table evolution from the Padul-15-05 record (proxies were resampled at 50 yr (lineal interpolation) using Past software http://palaeo-electronica.org/2001_1/past/issue1_01.htm). [(a.1) Magnetic Susceptibility (MS) in SI; (a.2) Silica normalized (Si; norm.); (a.3) Calcium normalized (Ca; norm.); (a.4) Bromine normalized (Br; norm.) ; (a.5) Strontium normalized (Sr; norm.); (a.6) Hygrophytes (%); (a.7) Poaceae (%); (a.8) Algae (%) (a.9) Total organic carbon (TOC %)] (b) Mediterranean forest taxa, with a smoothing of three-point in bold. Pink and blue shading indicates Holocene arid and humid regionally events, respectively. See the body of the text for the explanation of the lake level reconstruction. Mediterranean forest smoothing was made using Analyseries software (Paillard et al., 1996). CA = Copper Age; BA = Bronze Age; IA = Iron Age; IRHP = Iberian Roman Humid Period; DA = Dark Ages; MCA = Medieval Climate Anomaly; LIA = Little Ice Age; IE = Industrial Era.
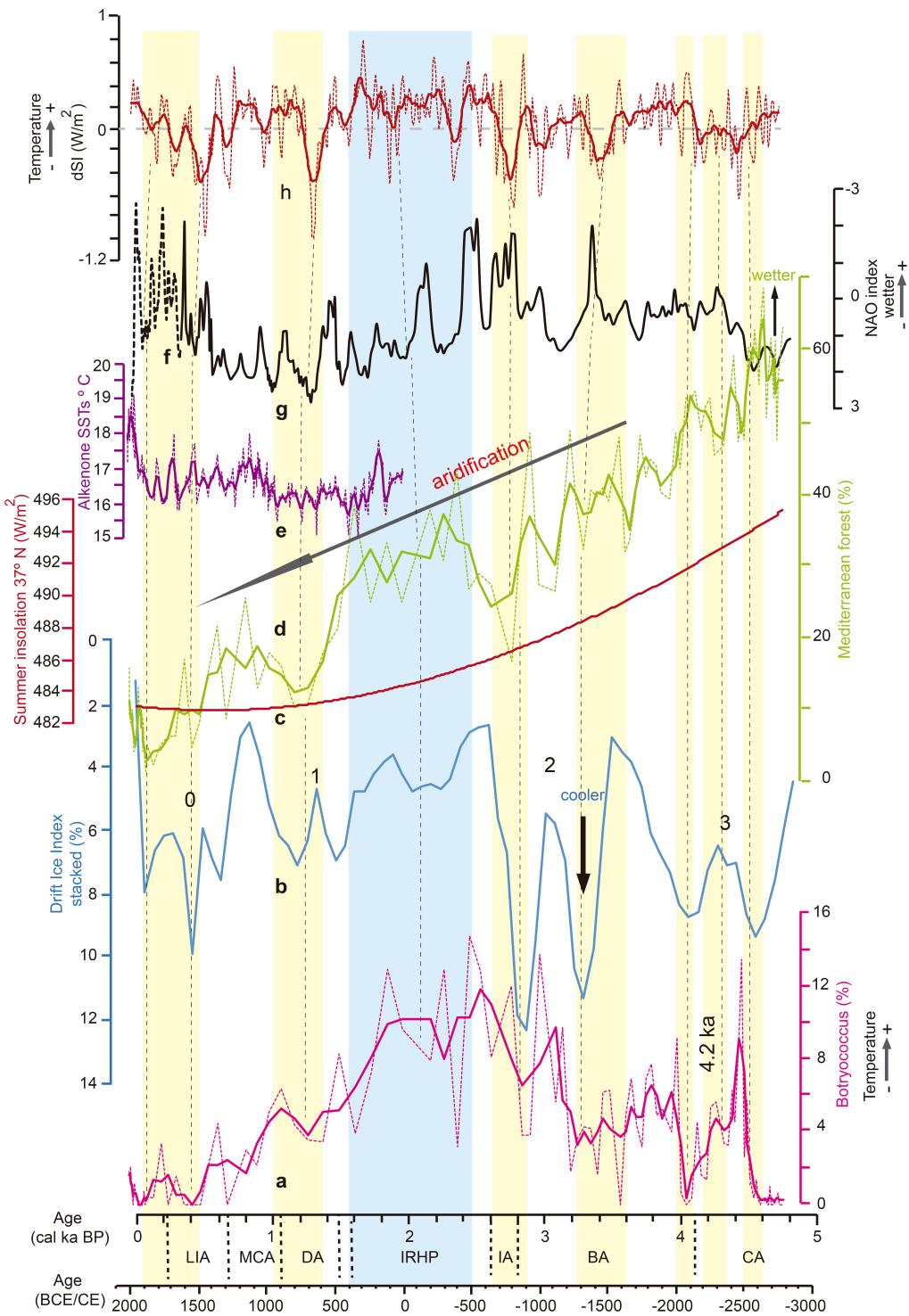
Figure 6. Comparison of the last ca. 4700 yr between different pollen taxa from the Padul-15-05 record, summer insolation for the Sierra Nevada latitude, eastern Mediterranean humidity and North Atlantic temperature. (a) *Botryococcus* from the Padul-15-05 record, with a smoothing of three-point in bold (this study). (b) Drift Ice Index (reversed) from the North Atlantic (Bond et al., 2001). (c) Summer insolation calculated for 37º N (Laskar et al., 2004). (d) Mediterranean forest taxa from the Padul-15-05 record, with a smoothing of three-point in bold (this study). (e) Alkenone-SSTs from the Gulf of Lion (Sicre et al., 2016), with a smoothing of four-point in bold. (f) North Atlantic Oscillation (NAO) index from a climate proxy reconstruction from Morocco and Scotland (Trouet et al., 2009). (g) North Atlantic Oscillation (NAO) index (reversed) from a climate proxy reconstruction from Greenland (Olsen et al., 2012). (h) Total solar irradiance reconstruction from cosmogenic radionuclide from a Greenland ice core (Steinhilber et al., 2009), with a smoothing of twenty-one-point in bold. Yellow and blue shading correspond with arid (and cold) and humid (and warm) periods, respectively. Grey dash lines show a tentative correlation between arid and cold conditions and the decrease in the Mediterranean forest and *Botryococcus*. Mediterranean forest, *Botryococcus* and solar irradiance smoothing was made using Analyseries software (Paillard et al., 1996), Alkenone-SSTs smoothing was made using Past software (http://palaeo-electronica.org/2001_1/past/issue1_01.htm). A linear r (Pearson) correlation was calculated between *Botryococcus* (detrended) and Drift Ice Index (Bond et al., 2001; r = -0.63; $p < 0.0001$; between ca. 4700 to 1500 cal ka BP – r=-0.48; $p < 0.0001$ between 4700 and -65 cal yr BP). Previously, the data were detrended (only in *Botryococcus*), resampled at 70-yr (linear interpolation) in order to obtain equally spaced time series and smoothed to three-point average. CA = Copper Age; BA = Bronze Age; IA = Iron Age; IRHP = Iberian Roman Humid Period; DA = Dark Ages; MCA = Medieval Climate Anomaly; LIA = Little Ice Age; IE = Industrial Era.
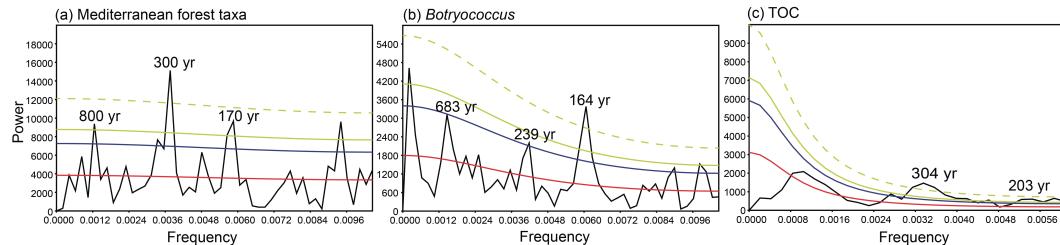
Figure 7. Spectral analysis of (a) Mediterranean forest taxa and (b) *Botryococcus* (mean sampling space = 47 yr) and (c) TOC (mean sampling space = 78 yr) from the Padul-15-05. The significant periodicities above confident level are shown. Confidence level 90 % (blue line), 95 % (green line), 99 % (green dash line) and AR (1) red noise (red line). Spectral analysis was made with Past software (http://palaeo- electronica.org/2001_1/past/issue1_01.htm).

1130   **Table 1.** Age data for Padul-15-05 record. All ages were calibrated using R-code package 'clam
1131   2.2' employing the calibration curve IntelCal 13 (Reimer et al., 2013) at 95 % of confident range.

1132   *Sample number assigned at radiocarbon laboratory

Laboratory number	Core	Material	Depth (cm)	Age (^{14}C yr BP ± 1σ)	Calibrated age (cal yr BP) 95 % confidence interval	Median age (cal yr BP)
Reference ages			0	2015CE	-65	-65
D-AMS 008531	Padul-13-01	Plant remains	21.67	103 ± 24	23-264	127
Poz-77568	Padul-15-05	Org. bulk sed.	38.46	1205 ± 30	1014-1239	1130
BETA-437233	Padul-15-05	Plant remains	46.04	2480 ± 30	2385-2722	2577
Poz-77569	Padul-15-05	Org. bulk sed.	48.21	2255 ± 30	2158-2344	2251
BETA-415830	Padul-15-05	Shell	71.36	3910 ± 30	4248-4421	4343
BETA-437234	Padul-15-05	Plant remains	76.34	3550 ± 30	3722-3956	3838
BETA-415831	Padul-15-05	Org. bulk sed.	92.94	3960 ± 30	4297-4519	4431
Poz-74344	Padul-15-05	Plant remains	122.96	4295 ± 35	4827-4959	4871
BETA-415832	Padul-15-05	Plant remains	150.04	5050 ± 30	5728-5900	5814
Poz-77571	Padul-15-05	Plant remains	186.08	5530 ± 40	6281-6402	6341
Poz-74345	Padul-15-05	Plant remains	199.33	6080 ± 40	6797-7154	6935
BETA-415833	Padul-15-05	Org. bulk sed.	217.36	6270 ± 30	7162-7262	7212
Poz-77572	Padul-15-05	Org. bulk sed.	238.68	7080 ± 50	7797-7999	7910
Poz-74347	Padul-15-05	Plant remains	277.24	8290 ± 40	9138-9426	9293
BETA-415834	Padul-15-05	Plant remains	327.29	8960 ± 30	9932-10221	10107

1133

1134

1135

1136

Table 2. Linear r (Pearson) correlation between geochemical elements from the Padul-15-05 record. Statistical treatment was performed using the Past software (http://palaeo-electronica.org/2001_1/past/issue1_01.htm).

	Si	K	Ca	Ti	Fe	Zr	Br	Sr
Si		8.30E-80	2.87E-34	7.47E-60	3.22E-60	5.29E-44	0.001152	7.79E-09
K	0.98612		7.07E-29	6.05E-60	8.20E-68	1.77E-51	0.00030317	5.38E-12
Ca	-0.88096	-0.84453		6.09E-42	5.81E-39	8.10E-34	0.35819	0.26613
Ti	0.96486	0.96501	-0.91794		1.74E-74	1.12E-57	0.074223	8.88E-07
Fe	0.96546	0.97577	-0.90527	0.98224		2.77E-66	0.051072	3.32E-08
Zr	0.92566	0.94789	-0.8783	0.96109	0.97398		0.054274	7.16E-08
Br	-0.31739	-0.3506	-0.091917	-0.17755	-0.19372	-0.19116		4.03E-18
Sr	-0.53347	-0.61629	0.11113	-0.46426	-0.51386	-0.50295	0.72852	